

NACA RM E57B26

CLASSIFICATION CHANGED

~~NACA UNCLASSIFIED~~

authority of STAR Date 3-31-71
U-9 No-1 Item 81/71

RESEARCH MEMORANDUM

PERFORMANCE AT HIGH TEMPERATURES AND PRESSURES
OF AN ANNULAR TURBOJET COMBUSTOR HAVING
ARTICULATED LINER WALLS

By Richard J. McCafferty, Jerrold D. Wear,
and William P. Cook

Lewis Flight Propulsion Laboratory
Cleveland, Ohio

LANGLEY RESEARCH CENTER
MAY 22 1957
LANGLEY RESEARCH CENTER
HAMILTON, VIRGINIA

CLASSIFIED DOCUMENT

This material contains information affecting the National Defense of the United States within the meaning of the espionage laws, Title 18, U.S.C., Secs. 793 and 794, the transmission or revelation of which in any manner to an unauthorized person is prohibited by law.

NATIONAL ADVISORY COMMITTEE FOR AERONAUTICS

WASHINGTON

May 10, 1957

~~CONFIDENTIAL~~

UNCLASSIFIED

UNCLASSIFIED

NACA RM E57B26



CLASSIFICATION CHANGED

NATIONAL ADVISORY COMMITTEE FOR AERONAUTICS

To _____ UNCLASSIFIED

RESEARCH MEMORANDUM

By authority of CSAR Date 3-31-71

PERFORMANCE AT HIGH TEMPERATURES AND PRESSURES OF AN ANNULAR

VA No. 1
lem
8-5-71

TURBOJET COMBUSTOR HAVING ARTICULATED LINER WALLS

By Richard J. McCafferty, Jerrold D. Wear, and William P. Cook

4378

SUMMARY

The performance of an experimental quarter-sector annular combustor was determined at conditions simulating supersonic flight of a cooled-turbine engine. Design features of the combustor configuration were aimed at providing a structurally strong, relatively cool operating liner that would give satisfactory combustion efficiency, pressure loss, and exhaust temperature pattern. The main design comprised many small parts, overlapping in construction, and independently suspended. Twenty modifications were tested.

The final configuration showed no structural failures and little or no warping of liner parts after about 40 hours of operation. Measured combustion efficiencies were over 100 percent at pressures of 25 pounds per square inch absolute and above for reference air velocities from 125 to 200 feet per second. Efficiency dropped to a minimum of about 92 percent when the pressure was lowered to 9.8 pounds per square inch absolute at a velocity of 160 feet per second. The total-pressure losses varied from 4.2 to 11.3 percent at an average exhaust temperature of 2000° F for reference velocities from 125 to 200 feet per second. Exhaust temperature patterns were reasonably uniform both radially and circumferentially.

INTRODUCTION

Higher airflows per unit frontal area and higher operating temperatures in turbojet engines aid in achieving the decreased specific engine weight necessary for higher altitudes and flight speeds. Increased air temperatures and airflows require engine components to function satisfactorily under greater mechanical and thermal stresses. Results of an investigation on an experimental turbojet combustion system having design features suited for operation at elevated gas temperatures and airflows are presented herein.

UNCLASSIFIED



Previous investigations at the NACA Lewis laboratory have demonstrated certain combustor design principles for operation at conditions representative of high-altitude supersonic flight (refs. 1 and 2). Combustion efficiencies between 85 and 100 percent were obtained in experimental combustors for pressures between $2/3$ and $1\frac{2}{3}$ atmospheres, outlet-gas temperatures of about 2000° F, and air reference velocities as high as 200 feet per second. These combustors were not operated at low-altitude higher pressure conditions where defects in structural durability would become apparent because of increased mechanical and thermal stresses.

Several combustor configurations similar to those reported in references 1 and 2 were built and tested at operating conditions that imposed a higher stress environment. In addition, a series of combustor configurations incorporating some new features aimed at increasing durability was also built and tested. In the latter configurations liner parts were segmented in both axial and circumferential directions and supported to the outer housing. Considerable cooling-air passage area through these segments was provided to maintain moderate metal temperatures. Individual pieces were allowed to expand freely to minimize stresses due to thermal gradients. Heat shields were provided to protect the outer housing walls at the exhaust end of the combustor.

Combustion performance and structural durability were evaluated at both high- and low-altitude supersonic-flight test conditions. Data are included herein to show combustion efficiencies, pressure losses, and outlet-gas temperature patterns at these test conditions and also to compare the performance of the final configuration with the performance of the combustor treated in reference 1. Other performance criteria, such as carbon deposition, are discussed. Details of the high-pressure facility required for the investigation are presented.

APPARATUS AND INSTRUMENTATION

Test Section and Installation

The combustor test section was connected to the laboratory air facilities as shown diagrammatically in figure 1. Air was drawn from the laboratory high-pressure supply system, passed through a counterflow tube heat exchanger into the test section, and exhausted into the altitude or atmospheric exhaust system. The heat exchanger was fed with exhaust products from four J47 combustors burning unleaded gasoline. Combustor inlet-air temperatures were controlled by means of a system that mixed bypassed air and air heated in the exchanger. The quantities of air flowing through the heater and its bypass system and the total pressure in the test section were regulated by remote-control valves.

The combustor test section and exhaust-gas instrumentation section were immersed in a water tank (fig. 1). This water bath was used to allow a reduction in weight and cost of these piping sections. Also, the exhaust instrumentation section had a replaceable inner liner of 3/32-inch-thick metal to protect the outer section from the hot exhaust gases. Since the facility was to be connected to compressors capable of supplying a pressure of 450 pounds per square inch, it was designed to withstand this maximum stress. The design also allowed a maximum average gas temperature of 2500° F.

A sketch of the combustor housing and inlet and outlet ducting is shown in figure 2. The combustor housing was a one-quarter sector of a single annular combustor with an outside diameter of $25\frac{1}{2}$ inches, an inside diameter of $10\frac{5}{8}$ inches, and a combustion length of about 23 inches. The maximum cross-sectional flow passage area was 105 square inches (420 sq in. for a complete annular housing). The inside dimensions of this housing were identical to those described in reference 1. Inlet and outlet ducting simulated the airflow passage of a particular full-scale engine having an axial-flow compressor and turbine. A punched plate containing 460 holes (1/4-in. diam.) which gave about 80 percent blockage of the pipe area was located in the flange just upstream of the inlet transition to smooth out irregularities in air velocity profile.

Instrumentation

The combustor instrumentation stations are shown in figure 2. Combustor inlet-air temperature was measured at station 1 by four closed-end chromel-alumel thermocouples. Location of the temperature- and pressure-measuring devices in the inlet duct is shown in figure 3. Inlet velocity pressures were measured at the same station with five rakes, each having three total-pressure tubes. The tubes were connected to strain gages that were balanced by wall static-pressure taps at station 1. Velocity pressure readings from the strain gages were recorded on a strip chart recorder. The wall static pressures were also indicated on Bourdon gages used to control the combustor inlet-air pressures.

Combustor outlet temperatures and pressures were measured at station 2 with a polar-coordinate traversing-probe mechanism that made five circumferential sweeps at radial centers of equal areas. The locations of these sweeps are shown in figure 4. A similar probe mechanism is described in reference 3. The probe had two measuring elements: a sonic aspirating-type platinum-13-percent-rhodium - platinum thermocouple and a total-pressure tube. A strain gage indicated the difference between the total pressure sensed at the probe end and the total pressure measured at the combustor inlet; the difference was considered to be the total-pressure drop across the combustor system. An X-Y automatic-balancing

potentiometer recorded a continuous trace of the temperature and pressure drop during circumferential motion of the probe.

Combustor outlet probes made of Inconel metal, such as described in reference 3, failed after a few surveys during runs where 2600° to 3000° F temperatures were encountered. The end of the tube burned away, and the pressure tube was thereby ruptured. A probe incorporating an all-platinum - 13-percent-rhodium tip was built in an effort to improve durability. The probe end, total-pressure tube, sonic nozzle, and about $1\frac{3}{4}$ inches of tubing were fabricated from platinum-13-percent-rhodium tubing; the tip was soldered to a jacketed water-cooled Inconel section. A photograph of this probe is presented in figure 5, and reference 4 presents additional details. The platinum-tip probe gave a longer service life; however, at the highest combustion pressure the probe was susceptible to steam vapor lock in the jacket, which resulted in rupture of the wall between the platinum and the Inconel sections. Consequently, the water pressure to the jacket was increased to avoid steam formation.

4378

Fuel

The fuel used in the investigation was MIL-F-5624A, grade JP-5 (NACA 54-35). The physical and chemical properties of the fuel are presented in table I.

PROCEDURE

Data were obtained at the following combustor test conditions:

Condition	Inlet-air total pressure, lb/sq in. abs	Inlet-air temperature, °F	Airflow, lb/sec	Reference velocity, ft/sec
A	9.8	860	2.35	160
B	14.7	↓	3.53	↓
C-1	25.0	↓	4.65	125
C-2	↓	↓	5.90	160
C-3	↓	↓	7.37	200
D	114.5	↓	20.8	110
E	205	660	33.7	95

Reference velocities are based on the maximum cross-sectional area of the combustor flow passage and on combustor inlet-air density. Conditions A, B, and C were taken from reference 1. Condition C-2 corresponds to an

engine with a compressor pressure ratio of 7 operating at a flight Mach number of 2.5 and an altitude of 70,000 feet. Conditions A and B were arbitrarily selected so that differences in combustion efficiency could be detected at lower pressures with a constant inlet-air velocity. Conditions C-1 and C-3 were used to ascertain velocity effects on performance at constant pressure. Conditions D and E were chosen to represent severe durability test conditions. Condition D corresponds approximately to an engine with a pressure ratio of 8 at Mach 2.5 and 35,000 feet.

4378

Combustor total-pressure losses, outlet temperature profiles, and combustion efficiencies were determined over a range of fuel-air ratios at each of the above conditions. Combustion efficiency was computed as the ratio of the measured enthalpy rise from inlet to outlet instrumentation planes to the theoretical enthalpy rise. The outlet-gas enthalpy was determined from the average outlet-gas temperature, which was obtained from the circumferential traces at each of the five radii. Values at 2° intervals on the circumferential traces, or a total of 215 temperatures, were averaged for each data point.

PRELIMINARY COMBUSTOR EVALUATIONS

The various combustor configurations are presented in two groups. The combustor described in reference 1 and three modifications were tested for durability; these combustors are called design I. Essential design features included long slots for air penetration, air-film cooling on the walls, and articulated sections to prevent warping and buckling. Other features are described in reference 1.

No data are reported for these combustors, because the traversing-probe mechanism was not installed during these tests, and the exhaust thermocouples used were insufficient in number to provide an accurate average temperature of the exhaust gases. A second group, called design II, constituted enough of a change in design to require a program of modifications aimed at improving other performance factors besides durability. These design II modifications are discussed collectively with regard to their structural makeup, and the various performance results obtained with them are presented separately. The performance of the final configuration is summarized and compared with the performance of the combustor of reference 1. The results obtained with design II combustors at all conditions tested are shown in table II. Inconel metal was used exclusively for both design I and II combustors.

A cutaway sketch of the design I combustor (from ref. 1) is shown in figure 6. This combustor has one-piece primary-zone liner walls for a length of 10 inches, while the secondary-zone walls are composed of 12 channel-shaped metal pieces attached between the downstream end of the

primary section and an exhaust heat shield. The fuel was injected through nine hollow-cone swirl-atomizing simplex nozzles (10.5 gal/hr flow capacity, 60° spray angle). This combustor liner was operated at condition C-2 for 1 hour with an average exhaust-gas temperature of about 2100° F. Failure of the liner pieces occurred, as shown by the photograph in figure 7.

The next design I liner tested is shown in figure 8. The one-piece primary-zone walls were 4.3 inches long; the remainder of the liner was composed of two sets of channel sections (12 sections in each set) supported to the outer housing walls by means of bolts located at the junction of the sets of channel pieces. Each channel piece was free to move longitudinally, since all fastenings were loose. This design did not fail during 1 hour of operation at test condition C-2, but did fail quickly at the higher pressure test condition D.

In the next modification of design I the metal thickness of the channels and the primary section was increased from 0.043 to 0.0625 inch. The cooling louvers were omitted from the channel pieces. Operation at condition D and an exhaust temperature of 1600° F for 2 hours gave the results shown in figure 9. Metal warping, especially in the upstream end of the combustor, was severe. This design was again tested after the warped surfaces were straightened and two metal reinforcing strips were welded edgewise to the side away from the flame zone of each channel piece. These metal strips were 1/16 inch thick and about 1 inch high. In an attempt to reduce thermal stresses in the primary zone this section was split into two 1/8 sectors. A side wall plate was welded on each sector at the cut end. Figure 10 shows the liner after 2 hours of operation at condition D and an exhaust temperature of about 1600° F. Again liner failure occurred, but warping was not as severe as in previous models. These durability tests indicated that more strength in each individual metal piece, less interdependence among the pieces for support, and cooler operating metal temperatures were required to increase liner life and eliminate warping. Major modifications were made to the combustor liner. These redesigned combustors were called design II configurations, and a complete evaluation of their aerothermodynamic performance was undertaken.

A photograph and a drawing representative of design II configurations are shown in figure 11. All configurations in this series were constructed of 1/16-inch-thick Inconel metal. The length of the combustor liner was about the same as design I combustors. The upstream end or pilot section was composed of two 1/8 sectors bolted to the fuel manifold. The inner and outer walls of the pilot section were composed of overlapping segments with supports between each segment. The channels were replaced with three smaller lengths of metal, herein called step-strips, welded together in an overlapping fashion with two longitudinal spacers between each length.

4378

The step-strips were supported from the outer walls as shown in figure 11(b) by three rows of bolts. Each step-strip was loosely held at each end and was not anchored to the pilot or downstream heat shield, as design I combustors were. Spacers were placed around the bolts to maintain the desired radial distance (with some tolerance for expansion) between the inner and outer walls. Design II combustors differed from design I combustors in that (1) the pilot section, the step-strips, and the heat shields were independently supported, (2) each individual piece was strengthened, and (3) considerable air flowed between each step to maintain lower metal temperatures. The plot presented in figure 12 shows the variation in cross-sectional flow area in the long- and short-radius dilution air passages, and in the cross-sectional area of the liner with distance along the combustor.

Six duplex nozzles were used for fuel injection, as shown in figure 11(b). These nozzles were designed to provide an atomized spray over the complete range of test conditions that might be encountered in determining the complete operational map of a supersonic engine with a compressor pressure ratio of 8. The fuel manifold was split into two passages so that the small-slot and large-slot systems of the nozzles were fed fuel independently, but each nozzle slot system did not receive fuel independently of the other nozzles.

Twenty different configurations of design II combustors were tested. Table III presents a summary of these different configurations; the locations of zones A, B, C, D, and E are shown in figure 2. Since most of the configuration changes were aimed at providing a more uniform exhaust temperature profile or reducing combustor pressure losses, the changes, in general, consisted of variations in the width and length of air-admission holes in the downstream dilution zone. Total air-admission area was varied from 101.5 to 37.8 square inches. The ratio of air-admission area in the outer wall to the air-admission area in the inner wall of the liner varied from 0.5 in configuration 2 to 3.0 in configuration 19. Variations in open area in the liner were generally in the downstream half, while the first half of the liner was held reasonably constant. Curves showing the variation in air-admission hole area with distance downstream from the fuel manifold face are presented in figure 13 for four representative configurations. The proportion of air-admission area in the first half of the combustion zone (about 11 in. of the upstream length) to total air-admission area varies from 33 percent (configuration 1) to 85 percent (configuration 11).

Durability Characteristics of Design II

A photograph of configuration 20 is presented in figure 14. This photograph was taken after about 40 hours of operation at various test conditions. The pilot section and upstream set of step-strips are the

original ones; the downstream step-strips were replaced during the program because of the many cuts and rewelds necessary for the various configurations. No appreciable warping or cracks in the liner parts occurred. Four different tabs attached to the ends of the bolts supporting the step-strips were lost during the program; no attempt was made to improve the structural integrity of these tabs.

Configuration 20 was operated at condition D for about 20 hours with a 2000° F or higher average outlet-gas temperature. Exhaust-gas temperature patterns that were recorded at the start and end of this 20-hour test are shown in figure 15. Temperatures recorded at five radii show that no appreciable change in outlet temperature pattern, either radial or circumferential, occurred. Structurally, then, design II configurations were quite satisfactory, but an improved method of attaching tabs to the support bolt ends appears necessary.

4378

Combustion Efficiency of Design II

Combustion efficiency values are shown in figure 16 for test conditions A and B and test runs where the average exhaust-gas temperature was between 1800° and 2100° F. The abscissa scale is the ratio of air-admission area in the liner to the maximum cross-sectional area of the outer housing. Data were not obtained with all the configurations at both test points. In general, measured combustion efficiencies were high, ranging from 85 to 98 percent at condition B and from 85 to 94 percent at condition A.

Similar efficiency performance could be then obtained, regardless of air-admission open area within the range investigated. This can be explained by considering the relative effectiveness of the air passages between the steps in the liner strips and the air passages (slots) between the strips. For a given amount of area, the openings formed by the steps would be expected to flow a larger quantity of air than the slots between the strips, because the step openings are normal to the flow direction while the slots are inclined at an angle to the flow direction. Experimental data indicate that the discharge coefficient of the step openings is about 0.8, while the coefficient of the slots ranges from about 0.6 at the downstream end to about 0.2 at the upstream end of the combustor. The open area formed by the step openings was not changed appreciably during the configuration changes, and, also, a large portion of unchanged area was located in the pilot section (table III). This means the effective area and amount of primary air varied much less than is indicated by the range of abscissa values in figure 16. Such combustor designs with a high percentage of the total airflow introduced into the primary zone would probably not be able to maintain satisfactory combustion efficiencies at extremely low pressures such as might be encountered in a low-pressure-ratio engine operating subsonically at extreme altitudes. For supersonic flight with high-compression engines, however, this design

idea seems quite attractive from the viewpoint of shorter combustor length, lower combustor weight, and better structural durability.

4378

Table II presents combustion efficiency values as high as 108 percent; these values were calculated using the arithmetical average combustor exhaust temperature. It was thought that, if appropriate corrections were made to the thermocouple probe indications to allow for variation in mass flow across the exhaust duct, these efficiency values would be more nearly correct. Reference 5 presents efficiency values corrected in this manner that were lowered by as much as 8 percent. Mass-weighted average temperatures were calculated for two test runs using the total-pressure tube reading in the probe at corresponding 2° intervals and assuming constant static pressure across the exhaust duct. The variation in air mass flow with angular position in the duct for the five radii is shown in figure 17 for a representative test run. The curves in figure 17 are extrapolated to the side walls. The efficiency calculated from arithmetically averaged exhaust temperatures was 103.7. For this run, the mass-weighted average outlet temperature was lowered slightly, and the corrected combustion efficiency was 102 percent. For the second test run where the uncorrected efficiency was 107.1 percent, mass weighting lowered the efficiency value less than 1 percent. Mass weighting, then, did not appreciably affect computed combustion efficiency values in the design II combustors, as the exhaust mass-flow patterns in the area covered were reasonably uniform. A possible source of error is the amount of gases in the area along the four walls not swept by the probe. Also, errors in the computed efficiency values could be due to accumulated measurement errors in airflow orifices, fuel measuring devices, and thermocouple probes, although these devices were frequently checked during the investigation.

Pressure Losses of Design II

Total-pressure loss, in percent of inlet total pressure, is shown in figure 18 as a function of the ratio of air-admission area to maximum cross-sectional area of the combustor housing. Data are shown for the various configurations operated at condition B with average exhaust-gas temperatures between 1700° and 2100° F. Total-pressure loss varied from 5.8 to 7.3 percent for the various configurations; in general, pressure loss increased with a decrease in the air-admission area. Tests conducted at condition B without burning showed that the duct alone, without fuel manifold or liner, gave about 2 percent pressure loss; and with manifold and pilot section installed, about 3 percent. Since momentum pressure loss due to combustion would be expected to be slightly greater than 1 percent, the remainder of the loss (about 3 percent) is apparently due to the step-strip configuration. The exact amount of loss chargeable to the liner configuration is not known, since the loss characteristics of the housing and manifold may be altered with the liner installed.

A number of the configuration changes were made in an effort to reduce pressure losses (i.e., configurations 12 to 20). The modifications incorporated in configurations 12 to 20 were not considered successful with regard to pressure losses, since the exhaust temperature pattern was adversely affected. Changes made to reestablish a satisfactory pattern resulted in the final configuration, which had about the same pressure loss characteristics as configuration 11.

Removal of the spacer pieces surrounding the support bolts and replacing them with a thin lock nut, so that the area blockage in the dilution air passage was less, resulted in decreasing the pressure loss about 1/2 percent at condition B (compare configurations 14 and 15 in fig. 18).

Pressure loss values of 6 to 7 percent are not considered excessive for turbojet combustion systems at air reference velocities of the order of 160 feet per second and outlet temperatures of 2000° F, which are about the most severe conditions from a pressure loss viewpoint to be encountered in an engine of this type. These losses, which might be considered acceptable for this type of engine, would result in effects on thrust and specific fuel consumption similar to those encountered in current turbojet engines. Improved diffuser and fuel manifold design together with a method of attachment of the step-strips that would cause less blockage would probably result in some decrease in pressure losses.

Exhaust Temperature Pattern of Design II

Configurations 1 to 11 were aimed specifically toward obtaining a uniform outlet temperature pattern, flat in a radial direction and without excessive peaks and dips circumferentially. As mentioned previously, the subsequent modifications (configurations 12 to 20), were aimed at reducing pressure losses without spoiling the temperature pattern. Exhaust temperature patterns for selected configurations are shown in figure 19. The exhaust temperature patterns obtained with configuration 1, which are not shown in figure 19, had excessive dips at both long and short radii, which indicated that the area between the two pilot sections had to be closed. Configuration 2 (fig. 19(a)) had excessive circumferential peaks and valleys at the long-radii positions. Table II shows that the outer-wall slots were about half the area of the inner-wall slots; therefore, the air was coming through the outer-wall slots with excessive velocity and did not spread sufficiently, and alternate hot and cold layers resulted.

The pattern for configuration 4 (fig. 19(b)) showed very low temperatures at the long and short radii (turbine blade tip and root positions). The area underneath the heat shields (combustor zone E) was closed in configuration 4A, and the resulting temperature pattern (fig. 19(c)) exhibited a much flatter radial profile. In configuration 6 four extra slots were made in the middle of the step-strips on each radius; the

4378

pattern obtained (fig. 19(d)) shows the turbine blade root temperature was too low, while the temperatures in the middle radii were excessively high. The excessive slot area resulted in insufficient penetration, and the pattern is cold near the wall with a hot core down the middle of the duct. In configurations 7 to 11 the slot area between the downstream step-strips (zone D) was reduced. The temperature pattern for configuration 11 (fig. 19(h)) shows a reasonably good circumferential and radial temperature distribution. A graph showing an exhaust temperature pattern factor for each of the configurations is presented in figure 20. These data were obtained at condition B with exhaust average temperatures of 1800° to 2150° F. The temperature factor used is the maximum temperature recorded in 80° of the probe sweep minus the average temperature divided by the temperature rise through the combustor. Since these data were obtained in the same general range of average temperature and temperature rise values, the factors shown are almost directly associated with the maximum recorded temperature. A successive improvement in exhaust pattern can be noted in figure 20 where the temperature factor was, in general, reduced with each configuration change through 11. The total area of air-admission openings was reduced from about 90 to about 38 square inches through these changes. A comparison of area plotted against combustor length between configurations 1 and 11 (fig. 13) shows that the upstream half of the burner was not materially modified, while in the downstream half the slot area was practically eliminated. The elimination of the slots in the downstream region forced more of the dilution air to enter near the upstream end of the liner and allowed the hot and cold gases to mix over a greater length, which resulted in better exhaust temperature patterns.

As mentioned previously, configurations 12 to 20 were aimed at reducing pressure losses without adversely affecting the outlet temperature pattern. Square holes were cut into the step-strips midway along the burner length to increase the open area and still allow a reasonable length for mixing. The temperature factor (fig. 20) increased in modifications 12 to 14 and then decreased again. The air-admission areas of configurations 15 to 20 were successively reduced; configuration 20 was similar to 11 in both exhaust temperature pattern and total open area.

Since all of the configurations were tested at condition B, effects of air-admission openings on exhaust temperature pattern are based on performance at this condition. However, the distribution appeared to be adversely affected by increased combustion pressure; the temperature factors obtained with configurations 11 and 20 at higher pressures were higher than those at the lower pressures (table II). Size and number of dilution air slots for a given liner surface were found to be important in this investigation (as well as in previous ones, refs. 1 and 2). Too few slots can cause alternating hot and cold stratification circumferentially, while too many can result in a distribution that is cold at blade root and tip positions and excessively hot along the center. A minimum

amount of air should be used to cool the exhaust walls and heat shields, since this bypassed air will not enter the mixing process before the turbine. For the particular combustor configurations tested herein the most uniform distributions were obtained by reducing liner open area, especially in the downstream half of the liner, and allowing a greater length for mixing. Obviously, if this technique is carried to an extreme, low combustion efficiencies (especially at low air pressures) and excessive pressure losses would result.

Fuel-System Characteristics of Design II

The six duplex nozzles used for fuel injection were mounted so that each had in common with the other nozzles two manifold passages, one passage for the small-slot and one for the large-slot systems. These two manifold passages could be fed fuel independently. Clogging of the small-slot passages of one nozzle in a manifold arrangement of this type results in an extremely unbalanced fuel distribution with that particular nozzle injecting nearly all the fuel supplied through its large-slot system. Clogging probably accounts for the extremely hot spot along the right wall for the test run with configuration 4 (fig. 19(b)). The hot spot is also reflected in a high value of the temperature pattern factor for this run (fig. 20). Several times during the course of the test program the duplex nozzles and the manifold were inspected and cleaned to avoid poor fuel distributions.

Data were obtained with several configurations at condition B with the fuel injected through the small nozzle slots only or through the large slots only. The amount of fuel required at condition B to produce an average exhaust temperature of 2000° F resulted in about a 30-pound-per-square-inch differential pressure with small-slot operation. Fuel spray checks into quiescent air showed that the small-slot system produced a complete 90° angle atomized spray at this pressure differential. No spray was produced with the same flow quantity with the large slots only. The exhaust temperature pattern factor obtained at test condition B for the configuration where data were obtained with the nozzles injecting fuel through the large slots only is presented in figure 21. The dotted line represents similar data from figure 20, obtained with the nozzles injecting fuel through small slots only. The data points for the large-slot injection fall on both sides of the dotted line with no consistent trend shown. The single triangular symbol for configuration 11B represents data obtained with six simplex nozzles (4.5 gal/hr flow capacity; 80° spray angle). This combination gave the lowest temperature pattern factor recorded during the test program. Exhaust temperature patterns are shown in figure 22 for small-slot and large-slot operation at test condition B with configuration 20. Neither the radial nor the circumferential profile reflects any significant effect of the variation in fuel-injection characteristics.

Combustion efficiencies were not markedly affected by switching from one slot system to the other. The average temperatures for both runs in figure 22 are the same. Inspection of the data presented in table II shows little difference in efficiency obtained with any of the configurations by switching slot systems. Hence, fuel atomization and distribution can be said to influence exhaust temperature distribution in these design II configurations but not in any predictable manner, and apparently the combustion efficiency of these combustors is not affected by atomization for the range of conditions tested.

A possible explanation is that about 10 percent of the total open area is included in the row of holes on the upstream long- and short-radius sides of the pilot section. These holes direct air around the nozzles beneath the nozzle protector plate, and the air issuing from these holes in the plate helps to atomize the fuel, even at low fuel flows where the nozzle is not providing a fine spray. Also, the axial sheets of air issuing from the steps in the pilot sweep unatomized liquid fuel from the walls, vaporize it, and mix it with air.

Coke Deposition in Design II Combustors

Coke was deposited in these combustors in small amounts on the surface of the nozzle protector plate (fig. 11(a)). Practically none was formed on the pilot section or liner parts. The absence of coking was due to the large amount of cooling air flowing along the metal surfaces through the steps and also due to the high inlet-air temperatures at the conditions tested. High inlet-air temperatures result in high metal temperatures throughout the combustor, and coke does not form on the hot metal (ref. 6). Considerable amounts of smoke were formed in the exhaust gases, especially at the higher pressure test conditions.

Considerable coke was formed from the fuel in the fuel manifold and nozzles. The nozzle clogging mentioned previously was largely due to this coke formation. Special operating procedures were used to reduce the fuel soaking period in the manifold and nozzles while these parts were hot. The test combustor was ignited before the inlet-air temperature was raised above 350° to 400° F in order to keep fuel flowing through these parts. The test combustor was shut down only after the inlet temperature was reduced to 300° F or less. This procedure did not eliminate coke formation, but did cut down the amounts formed and allowed a longer operating period between cleanings of the manifold and nozzles. It will be necessary to recognize this fuel coking problem in supersonic engine fuel systems. Design procedures such as keeping a minimum fuel volume in fuel-system components exposed to high temperatures should help alleviate this problem.

PERFORMANCE OF BEST CONFIGURATION

The final configuration (configuration 20) was chosen for further tests to determine combustion efficiency, pressure loss, temperature pattern, and durability over a wider range of operating conditions. This configuration was not the best in all respects, and the choice necessarily involved compromise. Configuration 20 provided the highest efficiency and showed satisfactory temperature profile and durability characteristics. Its pressure losses were, however, higher than those for many of the other configurations. Details and dimensions of configuration 20 are presented in figure 23.

Combustion Efficiency

The variation in combustion efficiency with fuel-air ratio for configuration 20 is shown in figure 24 for all the test conditions. Dotted lines representing constant temperature rise values are included on the plots. Data are shown for three methods of fuel injection: small slots only, large slots only, and both slots simultaneously. No attempt was made to control the amount of fuel proportioned to each slot system when both systems were used simultaneously. Measured combustion efficiencies varied from over 100 to 92 percent for inlet-air pressures from 9.8 to 204.5 pounds per square inch absolute at reference air velocities as high as 199 feet per second (at inlet-air pressure of 24.9 lb/sq in. abs). At the two lowest pressure conditions investigated, combustion efficiency varied from 92 to 98 percent over a temperature rise range of 650° to 1250° F, which would be expected to encompass engine operation from cruise to full-throttle. Variation of the fuel-injection slot system apparently had little effect on efficiency. This indicates that fuel atomization is not of paramount importance with this combustor design.

Combustion efficiencies obtained with configuration 20 and with the combustor system reported in reference 1 over a range of inlet-air pressure and reference velocity are compared in figure 25. These data were obtained at an average outlet-gas temperature of about 2000° F. Efficiencies obtained with configuration 20 are comparable or slightly superior to those obtained with the reference combustor at all the conditions tested. Efficiencies with configuration 20 were less sensitive to decreasing pressures (fig. 25(a)); efficiencies in both combustors were not significantly affected by variations in reference velocity from 125 to 200 feet per second at a pressure of 25 pounds per square inch absolute (fig. 25 (b)).

Pressure Loss

The pressure losses of configuration 20 and of the combustor of reference 1 are compared in figure 26. Pressure loss in percent of inlet total pressure is shown as a function of reference velocity at a pressure

of 25 pounds per square inch absolute (test condition C) and an average exhaust-gas temperature of about 2000° F. The pressure loss for configuration 20 increased from 4.2 to 11.3 percent over the range of velocities investigated. These losses are about one-third greater than those reported for the reference combustor.

Exhaust Temperature Pattern

4378 Representative exhaust temperature distributions obtained in three different runs with configuration 20 are shown in figures 15 and 22. The average exhaust temperature pattern factor for all the runs listed in table II for configuration 20 is about 0.46. Thus, for an average outlet temperature of about 2000° F, and a temperature rise of 1200° F, the maximum temperature to be expected would be of the order of 2500° F. This maximum temperature would probably decrease if the pressure decreased below 1 atmosphere. The maximum temperature usually occurred in the center of the duct near the side walls with this final configuration. Elimination of the effects of these side walls in a full-scale combustor may be expected to lower this maximum temperature.

Combustor configuration 20 showed no significant warping or other structural defects during nearly 40 hours of operation, and more than half of this time was at an average exhaust-gas temperature in excess of 2000° F. Combustion efficiency, uniformity of outlet temperatures, and durability were better than those obtained at identical conditions with the experimental configuration of reference 1. Pressure loss values were about one-third higher, however.

CONCLUDING REMARKS

The experimental combustion system designed for operation at high inlet-air temperatures and flows common to supersonic engine operation encountered no major structural failures during the investigation. The pertinent design features established in the research included separation of the combustor liner into many small parts, overlapping arrangement of the metal pieces forming each part, and independent support of these parts to either the fuel manifold or combustor housing. Use of many small overlapping parts and independent suspension resulted in a structurally stronger, cooler operating liner that was durable and nonwarping.

Comparison of the weight of this liner configuration with a typical subsonic engine liner of about the same length and diameter shows a weight penalty would be involved. A full annular liner would weigh about 88 pounds as compared to 46 pounds for the typical subsonic model. No attempt was made to minimize the liner weight in the experimental configuration, and probably a reduction could be made without seriously affecting

durability by slightly reducing the 1/16-inch metal thickness used and by other minor modifications. Also, use of better high-temperature alloys than Inconel may permit a significant weight reduction.

For the range of supersonic conditions investigated, the other performance factors such as combustion efficiency, exhaust temperature pattern, and pressure loss were maintained at satisfactory levels. Measured combustion efficiencies were 92 to over 100 percent, and pressure loss values were 4.2 to 11.3 percent of the total pressure. For an average exhaust temperature of 2000^o F the peak temperature expected in the exhaust gases would be about 2500^o F. Coke deposition was no problem in the liner, but sufficient amounts formed within the fuel system to clog nozzle passages.

Lewis Flight Propulsion Laboratory
National Advisory Committee for Aeronautics
Cleveland, Ohio, March 5, 1957

REFERENCES

1. Zettle, Eugene V., and Friedman, Robert: Performance of Experimental Channeled-Wall Annular Turbojet Combustor at Conditions Simulating High-Altitude Supersonic Flight. I - U-Shaped Channel Walls for Secondary-Air Entry. NACA RM E54L21a, 1955.
2. Zettle, Eugene V., Norgren, Carl T., and Mark, Herman: Combustion Performance of Two Experimental Turbojet Annular Combustors at Conditions Simulating High-Altitude Supersonic Flight. NACA RM E54A15, 1954.
3. Friedman, Robert, and Carlson, Edward R.: A Polar-Coordinate Survey Method for Determining Jet-Engine Combustion-Chamber Performance. NACA TN 3566, 1955.
4. Glawe, George E.: A High-Temperature Combination Sonic Aspirated Thermocouple and Total-Pressure Probe. (To be published in Jet Prop.)
5. Norgren, Carl T., and Childs, J. Howard: Effect of Fuel Injectors and Liner Design on Performance of an Annular Turbojet Combustor with Vapor Fuels. NACA RM E53B04, 1953.
6. Butze, Helmut F., and Wear, Jerrold D.: Performance of a Tubular Turbojet Combustor at High Pressures and Temperatures. NACA RM E55A24, 1955.

TABLE I. - PROPERTIES OF MIL-F-5624A, GRADE
JP-5, FUEL (NACA 54-35)

Boiling range, °F	360 to 502
Specific gravity, 60°/60° F	0.815
Hydrogen-carbon ratio by weight	0.160
Net heat of combustion, Btu/lb	18,600
Aromatics, ASTM D875-46T, percent by volume	14.3
Aromatics, silica gel, percent by volume	13.7
Accelerated gum, mg/100 ml	5
Aniline point, °F	148.6
Smoke point, mm	23.3
Smoke volatility index	32.1

4378

CR-3

TABLE II. - TEST CONDITIONS AND DATA OBTAINED WITH DESIGN II COMBUSTORS

Config-uration	Test con-dition (a)	Combustor inlet-air total pressure, lb/sq in. abs	Combustor reference velocity, ft/sec	Combustor inlet-air temperature, t_p	Combustor outlet average temperature, t_p	Combustor temperature rise, t_p	Air-flow, lb/sec	Fuel-air ratio	Combustion effi-ciency, percent	Total-pressure loss, percent	Maximum outlet temperature, t_p	Outlet temperature factor, T_{max}/T_{av}	Total run time for each configuration, Hr Min		
														Ar	Hr Min
2	D(s)	114.37	108	715	1318	605	20.88	0.00898	99.1	---	1800	0.789	8 05		
	D(b)		712	1315	601	20.78	0.00895	99.3	---	1720	0.877				
	D(i)		715	1320	605	20.78	0.00895	100.0	---	1740	0.894				
	D(t)		715	1320	605	20.88	0.0125	102.6	---	2120	0.652				
	D(s)	109	714	1803	1089	20.75	0.01857	101.2	---	2570	0.704				
	D(i)		717	2028	1309	20.60	0.0205	100.3	---	3150	0.858				
	A(s)		162	865	2104	1259	2.382	0.02199	90.6	---	3100	0.805			
	A(s)		162	868	1904	1038	2.358	0.01745	93.6	---	2625	0.695			
	A(s)	14.71	160	855	1477	622	2.561	0.01028	91.7	---	1980	0.808			
	B(s)		161	855	1446	561	3.523	0.00915	95.9	---	1795	0.658			
	B(s)		162	860	2015	1155	3.522	0.01985	92.7	---	2945	0.805			
	B(s)		161	860	2009	1149	3.523	0.0200	91.6	---	2810	0.837			
3	A(s)	9.77	165	880	1484	584	2.382	0.00982	90.3	5.5	2020	0.952	6 40		
	A(s)		164	875	1861	986	2.370	0.01710	90.8	6.1	2630	0.779			
	A(s)		164	870	2084	1224	2.379	0.02159	91.8	6.6	3180	0.870			
	B(s)		161	860	1454	594	3.524	0.00924	97.0	5.7	1980	0.851			
	B(s)	14.7	165	875	1862	987	3.541	0.01596	96.9	6.0	2960	1.114			
	B(s)		163	870	2026	1156	3.545	0.01877	97.8	6.4	3180	0.983			
	B(i)		163	868	2018	1150	3.552	0.01881	97.1	6.4	3160	0.993			
	B(i)		162	865	---	---	3.537	---	---	---	---	---			
	B(s)	9.80	161	861	---	---	2.357	---	---	---	---	---			
	A(s)		162	869	1491	623	2.350	0.01086	87.4	6.0	2175	1.097			
	A(s)		162	865	1659	794	2.348	0.01407	87.4	6.0	2510	1.071			
	A(s)		162	869	1818	949	2.343	0.01729	86.4	6.1	2930	1.17			
B(s)	14.7	162	865	1429	564	3.533	0.00929	92.0	6.1	1970	0.959				
B(s)		162	865	1613	748	3.531	0.01254	91.7	6.1	2520	1.212				
B(s)		162	865	1808	943	3.542	0.01591	92.7	6.3	3140	1.412				
D		114.4	110	724	---	---	21.01	---	---	2.5	---	---			
D(s)	114.5	111	727	1314	587	21.10	0.0084	103.0	2.8	1920	1.032	9 30			
D(s)		111	726	1447	721	21.14	0.01075	100.4	2.9	2670	1.696				
D(i)		111	727	1437	710	21.13	0.01074	98.9	2.8	2580	1.328				
D(i)		112	729	1669	940	21.14	0.01432	100.1	2.9	2960	1.575				
B(s)	14.7	161	864	1369	505	3.530	0.00884	86.2	5.7	1860	0.972				
B(s)		162	865	1758	871	3.542	0.01526	89.0	5.9	2950	1.593				
B(s)		79	192	1512	1320	3.329	0.0214	80.6	3.2	3080	1.172				
B(s)		161	862	1577	515	3.535	0.00881	88.0	5.8	1780	0.782				
B(s)	162	860	1711	851	3.542	0.01525	88.9	6.1	2430	0.844					
B(s)		161	859	1890	1031	3.538	0.01854	88.0	6.3	2760	0.843				
4A	B	14.7	77	175	---	---	3.530	---	---	2.4	---		---	2 06	
	B(s)		76	178	779	601	3.522	0.01122	73.2	2.9	1420		1.086		
	B(s)		76	181	1124	993	3.520	0.01808	83.1	3.1	2150	1.088			
	B(s)		78	185	1357	1174	3.526	0.01975	85.9	3.3	2600	1.157			
	B(s)	14.7	77	176	1108	932	3.522	0.01605	82.1	3.0	2180	1.150			
	B(i)		78	177	1082	905	3.530	0.01801	79.7	3.0	2300	1.345			
	B(i)		77	177	1318	1141	3.521	0.01975	83.4	3.2	2730	1.237			
	B(s)		78	178	1318	1141	3.521	0.01975	83.4	3.2	2625	1.144			
	5	B	9.8	161	880	---	---	3.538	---	---	5.5	---	---		5 20
		A		163	860	---	---	2.375	---	---	5.8	---	---		
		A(s)		164	860	1742	882	2.400	0.01476	92.9	6.5	2420	0.766		
		A(s)		164	860	1993	1133	2.400	0.01948	92.6	6.7	2820	0.728		
A(s)		14.7	164	859	2016	1157	2.400	0.01956	94.2	6.6	2925	0.785			
B(s)			161	865	1447	582	3.520	0.00951	92.6	6.1	1840	0.875			
B(s)			161	865	1777	912	3.520	0.01493	95.1	6.3	2445	0.732			
B(s)			161	865	2099	1254	3.522	0.02091	94.6	6.6	2955	0.835			
B(i)		114.5	162	865	2108	1241	3.536	0.02075	95.8	6.5	3060	0.768			
B(i)			162	865	2250	1385	3.534	0.02338	96.1	6.7	3050	0.377			
D(s)			112	726	1141	415	21.27	0.00694	87.2	2.8	1430	0.696			
D(s)			111	721	1371	650	21.31	0.01036	93.5	3.0	1880	0.782			
D(s)	14.7	111	724	---	---	21.28	0.01237	---	3.0	---	---				
B		161	865	---	---	3.520	---	---	5.6	---	---				
B(s)		161	867	1466	589	3.522	0.00950	93.8	6.1	1920	0.787				
B(s)		161	866	1758	892	3.522	0.01491	93.2	6.3	2450	0.775				
B(s)	14.7	161	864	2001	1137	3.522	0.01971	91.9	6.5	2870	0.803				
B(i)		161	865	1949	1084	3.520	0.01972	87.4	6.5	2670	0.665				
B(s)		161	866	1476	610	3.520	0.01013	91.4	6.1	1950	0.777				
B(s)		161	866	1708	840	3.520	0.01485	88.0	6.3	2320	0.730				
B(s)	14.7	162	866	1920	1054	3.534	0.01985	85.3	6.5	2605	0.649				
B(s)		162	866	1928	1060	3.530	0.01966	85.8	6.5	2520	0.560				
B(i)		162	865	1493	628	3.524	0.01011	94.1	5.9	1900	0.648				
B(i)		161	864	1752	868	3.532	0.01478	93.4	6.2	2380	0.707				
7A	B(s)	14.7	162	866	1955	1089	3.540	0.01866	81.6	6.4	2655	0.642	5 55		
	B(s)		162	866	2018	1152	3.540	0.01866	97.1	6.3	2640	0.340			

(s) denotes small nozzle slots only; (i) denotes large nozzle slots only; (b) denotes both large and small nozzle slots.

TABLE II. - CONTINUED. TEST CONDITIONS AND DATA OBTAINED WITH DESIGN II COMBUSTORS

Config-uration	Test condition (a)	Combustor inlet-air total pressure, lb/sq in. abs	Combustor reference velocity, ft/sec	Combustor inlet-air temperature, °F	Combustor outlet average temperature, °F	Combustor temperature rise, °F	Air-flow, lb/sec	Fuel-air ratio	Combustion efficiency, percent	Total-pressure loss, percent	Maximum outlet temperature, °F	Outlet temperature factor, $\frac{T_{max}-T_{av}}{T_{max}-T_{in}}$		Total run time for each configuration	
												Ar	Min	Hr	Min
8	B(s)	14.7	162	868	1454	586	3.543	0.00999	88.9	5.6	1845	0.667	1	55	
	B(s)		162	867	1714	847	3.538	.01477	89.2	5.8	2400	.809			
	B(s)		---	867	1900	1033	3.535	.01889	88.7	---	2800	.871			
	B(i)		---	867	1894	1027	3.538	.01888	88.2	---	2550	.838			
9	B(s)	14.7	161	865	1482	617	3.516	.01021	91.8	5.7	1950	.759	1	50	
	B(s)		162	866	1743	877	3.538	.01471	92.7	5.9	2430	.783			
	B(s)		162	865	1944	1079	3.533	.01891	90.5	6.1	2770	.765			
	B(i)		162	866	1915	1049	3.540	.01886	88.3	6.2	2700	.748			
9A	B(s)	14.7	162	867	1479	612	3.538	.01008	92.1	5.6	1900	.687	1	50	
	B(s)		163	867	1735	868	3.547	.01468	92.0	5.8	2325	.679			
	B(s)		163	865	1940	1075	3.532	.01882	90.6	6.0	2800	.813			
	B(i)		164	865	1920	1055	3.573	.01866	89.4	6.1	2620	.683			
10	B(s)	14.7	162	864	1488	624	3.540	.01008	93.9	5.7	1920	.683	1	45	
	B(s)		163	866	1755	889	3.554	.0147	94.1	5.9	2320	.655			
	B(s)		162	865	1961	1096	3.540	.01888	92.2	6.1	2700	.674			
	B(i)		163	865	1963	1098	3.557	.01877	92.8	6.1	2690	.662			
11	B(s)	14.7	162	865	1484	619	3.536	.01008	93.1	6.9	1850	.581	1	45	
	B(s)		162	865	1745	880	3.542	.01475	92.8	7.0	2025	.518			
	B(s)		162	865	1950	1085	3.540	.01880	91.6	7.3	2430	.442			
	B(i)		162	865	1957	1092	3.539	.01888	91.8	7.2	2560	.569			
11A	B	14.7	162	865	2100	1256	3.539	.02188	90.8	7.5	2550	.564	1	45	
	A		162	865	---	---	3.540	---	---	6.6	---	---			
	A(s)		162	861	---	---	2.363	---	---	6.7	---	---			
	A(s)		162	865	1554	689	2.368	.01158	92.5	7.2	1840	.415			
11B	A(s)	14.7	162	865	1874	1009	2.368	.01750	90.8	7.6	2280	.402	4	20	
	A(s)		163	865	2074	1209	2.370	.02197	88.5	7.8	2550	.583			
	B(s)		162	865	1482	617	3.533	.01009	92.8	7.0	1710	.569			
	B(s)		162	865	1745	880	3.536	.01472	92.9	7.4	1225	.431			
11C	D(s)	114.3	162	866	2001	1135	3.533	.01985	92.0	7.4	2470	.415	4	20	
	D(s)		110	725	1181	456	20.92	.00639	103.0	3.4	---	---			
	D(s)		110	725	1509	784	20.92	.01122	104.7	3.5	1950	.562			
	D(i)		110	726	1698	872	20.98	.01236	106.6	3.5	2030	.485			
11D	D(i)	114.3	---	---	---	---	---	---	---	---	---	---	4	20	
	D(i)		---	---	---	---	---	---	---	---	---	---			
	D(i)		---	---	---	---	---	---	---	---	---	---			
	D(i)		---	---	---	---	---	---	---	---	---	---			
11E	D(i)	114.3	---	---	---	---	---	---	---	---	---	---	4	20	
	D(i)		---	---	---	---	---	---	---	---	---	---			
	D(i)		---	---	---	---	---	---	---	---	---	---			
	D(i)		---	---	---	---	---	---	---	---	---	---			
11F	B	14.7	162	865	1484	619	3.540	.01005	93.4	---	1750	.430	1	30	
	B		162	865	1764	899	3.538	.0147	95.0	---	2055	.525			
	B		162	865	2150	1285	3.539	.0218	94.8	---	2510	.280			
	B		---	---	---	---	---	---	---	---	---	---			
12	B	14.7	162	863	---	---	3.533	---	---	5.5	---	---	2	25	
	A		163	863	---	---	2.372	---	---	5.7	---	---			
	A(s)		162	866	1624	758	2.356	.01337	86.2	6.2	1870	.325			
	A(s)		161	864	1858	994	2.362	.01809	88.5	6.4	2370	.515			
12A	A(s)	14.7	161	864	2112	1248	2.347	.02218	90.6	6.6	2760	.519	2	25	
	B(s)		162	868	1490	622	3.530	.01008	93.6	8.2	---	---			
	B(s)		163	867	1761	894	3.555	.0147	94.6	8.4	2140	.423			
	B(s)		163	867	2135	1266	3.544	.02162	93.5	6.8	2760	.493			
13	B	14.7	162	867	---	---	3.531	---	---	6.3	---	---	4	05	
	A		159	864	---	---	2.323	---	---	6.4	---	---			
	B(s)		162	869	1489	620	3.536	.01006	93.6	6.7	---	---			
	B		161	865	---	---	3.528	---	---	6.1	---	---			
13A	A	14.7	162	862	---	---	2.358	---	---	6.0	---	---	4	05	
	B(s)		161	866	1498	632	3.527	.01011	94.9	6.6	1880	.604			
	B(s)		161	867	1776	909	3.516	.01487	95.2	6.8	2385	.669			
	B(s)		161	866	2039	1173	3.520	.01963	95.3	7.0	2795	.644			
13B	B(s)	14.7	162	863	2023	1160	3.544	.01965	94.0	7.1	2805	.674	4	05	
	B(s)		163	870	1503	633	3.540	.01007	95.4	6.3	1805	.477			
	B(s)		162	866	1767	901	3.534	.01473	95.1	6.6	2380	.658			
	B(s)		163	866	2019	1153	3.553	.01953	94.0	6.9	2500	.417			
13C	B(s)	14.7	163	868	1497	629	3.533	.01003	95.1	6.3	1775	.442	3	30	
	B(s)		163	865	1752	867	3.555	.01448	95.2	6.6	2195	.499			
	B(s)		163	864	2006	1142	3.533	.01944	93.5	6.9	2520	.450			
	B(s)		---	---	---	---	---	---	---	---	---	---			
13D	B(s)	14.7	162	866	1500	634	3.530	.01010	95.3	6.6	1780	.442	1	40	
	B(s)		162	866	1785	899	3.527	.01484	94.4	6.8	2185	.467			
	B(s)		162	866	2021	1155	3.526	.01970	93.4	7.0	2500	.415			
	B(s)		---	---	---	---	---	---	---	---	---	---			

^a(s) denotes small nozzle slots only; (i) denotes large nozzle slots only; (b) denotes both large and small nozzle slots.
^bSimplex fuel nozzles (flow capacity, 4.5 gal/hr; 80° spray angle).

4378 CR-3 back

TABLE II. - CONCLUDED. TEST CONDITIONS AND DATA OBTAINED WITH DESIGN II COMBUSTORS

Config-uration	Test con-dition (a)	Com-bustor inlet-air total pressure, lb/sq in. abs	Com-bustor reference velocity, ft/sec	Com-bustor inlet-air tempera-ture, t_p	Com-bustor outlet average tempera-ture, t_{op}	Com-bustor tempera-ture rise, Δt_p	Air-flow, lb/sec	Fuel-air ratio	Com-bus-tion effi-ciency, percent	Total-pres-sure loss, percent	Maximum outlet tempera-ture, t_{op}	Outlet tempera-ture factor, $\frac{t_{max} - t_{av}}{\Delta T}$	Total run time for each con-figuration					
													Hr	Min				
14	B	14.7	162	865	---	---	3.538	---	---	6.1	---	---	0.921	5	10			
	B(s)		161	865	1613	648	3.528	.01018	---	6.6	2110	.888						
	B(s)		162	866	1825	959	3.534	.01481	---	6.7	2675	.779						
	B(s)		162	866	2122	1256	3.531	.01967	---	6.9	3100	---						
15	B	14.7	162	867	---	---	3.530	---	---	5.4	---	---	.856	1	20			
	B(s)		162	867	1507	640	3.525	.01011	---	5.8	2055	.770						
	B(s)		162	868	1821	953	3.529	.01481	---	6.0	2555	.732						
	B(s)		161	865	2112	1247	3.529	.01968	---	6.2	3025	---						
16	B	14.7	162	863	---	---	3.540	---	---	5.8	---	---	.538	1	40			
	B(s)		161	865	1499	634	3.522	.01012	---	6.0	1840	.832						
	B(s)		161	864	1811	947	3.530	.01482	---	6.3	2410	.644						
	B(t)		162	867	2103	1240	3.532	.01977	---	6.4	2750	.522						
16A	B(b)	14.7	163	865	1504	639	3.560	.01001	---	6.5	2100	.933	.381	1	15			
	B(b)		163	866	1803	937	3.560	.01478	---	6.7	2275	.521						
	B(b)		163	867	2105	1238	3.550	.01960	---	6.9	2750	---						
16B	B(s)	14.7	162	868	1498	632	3.526	.01011	---	6.3	1780	.462	.540	2	10			
	B(s)		162	866	1797	931	3.528	.01475	---	6.4	2300	.857						
	B(s)		162	870	2095	1225	3.523	.01962	---	6.7	2900	.458						
	B(t)		162	868	2103	1237	3.539	.01967	---	6.7	2670	---						
17	B	14.7	162	867	---	---	3.530	---	---	6.1	---	---	.523	1	50			
	B(s)		162	867	1506	639	3.534	.01016	---	6.3	1840	.531						
	B(s)		162	866	1799	933	3.544	.01476	---	6.6	2295	.520						
	B(s)		161	865	2105	1240	3.508	.01978	---	6.7	2750	---						
18	B	14.7	162	864	---	---	3.542	---	---	6.2	---	---	.299	1	25			
	B(s)		162	865	1627	622	3.546	.01005	100.0	6.6	1725	.389						
	B(s)		162	865	1754	899	3.544	.01469	94.1	6.8	2100	.446						
	B(s)		162	865	2037	1172	3.534	.01965	95.0	6.9	2560	.457						
	B(t)		162	866	2022	1156	3.544	.01969	94.0	6.8	2550	---						
19	B	14.7	163	866	---	---	3.550	---	---	6.6	---	---	.491	1	10			
	B(s)		162	867	1505	636	3.526	.01011	94.9	6.9	1815	.634						
	B(s)		162	867	1766	899	3.530	.01482	94.4	7.2	2220	.505						
	B(s)		161	866	2022	1156	3.521	.01971	93.4	7.3	2755	---						
20	B	9.8	162	870	---	---	3.530	---	---	6.5	---	---	.449	38	35			
	B(s)		162	869	1508	639	3.527	.01010	98.1	7.0	1795	.375						
	B(s)		162	865	1786	921	3.534	.0148	96.8	7.0	2130	.402						
	B(s)		162	865	2038	1173	3.536	.01962	95.2	7.2	2510	.388						
	B(t)		162	866	2036	1170	3.534	.01963	94.9	7.2	2490	.453						
	B(t)		162	866	1781	915	3.532	.01461	96.1	7.0	2205	.393						
	B(t)		162	867	1621	654	3.537	.01016	98.3	6.8	1770	.450						
	A(s)		165	867	1634	769	2.406	.01225	96.4	7.1	1980	.376						
	A(s)		165	864	1926	1062	2.411	.01765	94.9	7.3	2325	.402						
	A(s)		165	865	2106	1241	2.400	.0217	91.9	7.4	2605	---						
	A		165	866	---	---	2.398	---	---	6.5	---	---						
C-1	C-1	24.94	125	866	---	---	4.623	---	---	5.6	---	---	.508	38	35			
	C-2		158	866	---	---	5.879	---	---	6.1	---	---						
	C-3		202	865	---	---	7.592	---	---	10.0	---	---						
	C-1(s)		125	865	1817	952	4.658	.01488	99.7	4.2	2300	.486						
C-1(s)	C-1(s)	24.94	125	866	1833	967	4.636	.01482	101.6	4.1	2300	.415	.488	38	35			
	C-1(s)		126	866	2093	1227	4.674	.01881	103.7	4.2	2600	.502						
	C-2(s)		159	866	1792	926	5.894	.01402	102.4	6.7	2350	.540						
	C-2(s)		159	866	2086	1220	5.918	.01868	103.7	6.9	2700	.486						
	C-2(t)		161	868	2076	1210	5.956	.01859	103.3	6.9	2730	.451						
	C-3(s)		199	865	1757	892	7.366	.01343	102.6	11.0	2200	.486						
	C-3(s)		199	866	2045	1180	7.366	.0160	103.7	11.3	2650	.512						
	D		110	726	---	---	20.90	---	---	2.7	---	---				.465	38	35
	D(s)		110	727	1271	544	20.88	.00769	103.8	2.9	1525	.468						
	D(s)		109	725	1287	562	20.78	.00775	106.5	3.0	1550	.534						
	D(s)		110	725	1440	715	20.84	.00993	107.1	3.1	1775	.433						
D(s)	111	726	1572	846	20.98	.01238	103.0	3.1	2075	---								
D(b)	111	727	1607	1080	21.03	.01596	104.2	3.1	2275	---								
D	---	727	---	---	21.14	.01912	---	---	---	---								
D(s)	114.4	110	728	1414	688	20.94	.00992	103.3	3.1	1725	.448							
D(b)	110	110	728	1812	1086	20.98	.01616	103.6	3.1	2300	.455							
D(b)	110	110	722	2012	1290	20.89	.01932	104.6	3.2	2600	---							
D(b)	114.1	111	722	---	---	20.90	.01948	---	3.3	---	---							
D(b)	D(b)	114.4	110	725	1866	1141	20.96	.01630	108.0	3.1	2500	.554	.450	38	35			
	D(b)		110	725	2051	1328	20.87	.01944	107.1	3.1	2650	---						
E	E	204.5	95	676	---	---	35.70	---	---	2.1	---	---	.570	38	35			
	E(b)		94	654	1597	745	33.82	.01018	107.7	2.2	1775	.508						
	E(b)		94	652	1531	699	33.63	.01024	100.6	2.1	1750	---						

(s) denotes small nozzle slots only; (t) denotes large nozzle slots only; (b) denotes both large and small nozzle slots.

TABLE III. - SUMMARY OF AIR-ADMISSION AREAS OF DESIGN II COMBUSTORS

Com- fig- ura- tion	Zone A		Zone B		Zone C				Zone D				Zone E		Area of slots between step- strips, sq in.	Area of slots between step- strips for cool- ing air, sq in.	Total ad- mis- sion area, sq in.
	Fuel nozzles	Size of holes in nose pro- tec- tor plate, in.	Open area be- tween pilot sec- tors, sq in.	Holes in strip between pilot sectors		Size of slit between pilot and end of step-strips, in.		Description of slots in primary set of step-strips (a)		Description of slots in secondary set of step-strips (a)		Size of slit between heat shield and walls of outer boning, in.					
				Num- ber	Size, in.	Outer combus- tor wall	Inner combus- tor wall	Outer combus- tor wall		Inner combus- tor wall		Outer combus- tor wall	Inner combus- tor wall				
								Num- ber	Size, in.	Num- ber	Size, in.			Num- ber			
1	First set of duplex	3/4	2.16	None		$\frac{1}{8} \times 1\frac{1}{2}$	$\frac{7}{16} \times 1\frac{1}{2}$	3 $b_{7\frac{3}{16}}$ 2 $d_{7\frac{1}{8}}$	3 $b_{7\frac{3}{16}}$ 2 $d_{7\frac{1}{8}}$	7 $7\frac{7}{16}$ 2 $d_{7\frac{1}{4}}$	3 $b_{7\frac{5}{4}}$ 2 $d_{7\frac{1}{2}}$	$\frac{5}{8} \times 20$	$\frac{1}{4} \times 9.8$	10.3	28.9	28.4	80.1
2	First set of duplex	3/4	0.1	8	1/8	$\frac{1}{8} \times 1\frac{1}{2}$	$\frac{7}{16} \times 1\frac{1}{2}$	3 $b_{7\frac{3}{16}}$ 2 $d_{7\frac{1}{8}}$	3 $b_{7\frac{3}{16}}$ 2 $d_{7\frac{1}{8}}$	4 $d_{7\frac{1}{16}}$ 2 $d_{7\frac{1}{4}}$	3 $b_{7\frac{3}{4}}$ 2 $d_{7\frac{1}{2}}$	$\frac{5}{8} \times 20$	$\frac{1}{4} \times 9.8$	10.0	18.7	40.2	89.7
3	First set of duplex	3/4	0.1	8	1/8	$\frac{1}{8} \times 1\frac{1}{2}$	$\frac{7}{16} \times 1\frac{1}{2}$	3 $b_{7\frac{3}{16}}$ 4 $d_{7\frac{3}{32}}$	3 $b_{7\frac{3}{16}}$ 2 $d_{7\frac{1}{8}}$	7 $7\frac{7}{16}$ 2 $d_{7\frac{1}{4}}$	3 $b_{7\frac{5}{4}}$ 2 $d_{7\frac{1}{2}}$	$\frac{5}{8} \times 20$	$\frac{1}{4} \times 9.8$	9.6	31.5	40.2	101.3
4	First set of duplex	3/4	0.1	8	1/8	$\frac{1}{8} \times 1\frac{1}{2}$	$\frac{7}{16} \times 1\frac{1}{2}$	5 $b_{7\frac{3}{16}}$ 4 $d_{7\frac{3}{32}}$	3 $b_{7\frac{3}{32}}$ 2 $d_{7\frac{1}{16}}$	7 $7\frac{7}{16}$ 2 $d_{7\frac{1}{4}}$	3 $b_{7\frac{5}{4}}$ 2 $d_{7\frac{1}{2}}$	$\frac{5}{8} \times 20$	$\frac{1}{4} \times 9.8$	10.3	31.5	28.2	90.1
4A	Second set of duplex	3/4	0.1	8	1/8	$\frac{1}{8} \times 1\frac{1}{2}$	$\frac{7}{16} \times 1\frac{1}{2}$	5 $b_{7\frac{3}{16}}$ 4 $d_{7\frac{3}{32}}$	3 $b_{7\frac{7}{32}}$ 2 $d_{7\frac{1}{16}}$	7 $7\frac{7}{16}$ 2 $d_{7\frac{1}{4}}$	3 $b_{7\frac{3}{4}}$ 2 $d_{7\frac{1}{2}}$	Closed	Closed	10.3	31.5	28.2	80.2
5	Second set of duplex	3/4	0.1	8	1/8	$\frac{1}{8} \times 1\frac{1}{2}$	$\frac{7}{16} \times 1\frac{1}{2}$	5 $b_{7\frac{3}{16}}$ 4 $d_{7\frac{3}{32}}$	3 $b_{7\frac{3}{4}}$ 2 $d_{7\frac{1}{8}}$	7 $7\frac{7}{16}$ 2 $d_{7\frac{1}{4}}$	3 $b_{7\frac{5}{4}}$ 2 $d_{7\frac{1}{2}}$	Closed	Closed	10.3	31.5	28.2	80.2
6	Second set of duplex	3/4	0.1	8	1/8	$\frac{1}{8} \times 1\frac{1}{2}$	$\frac{7}{16} \times 1\frac{1}{2}$	3 $b_{7\frac{3}{16}}$ 4 $d_{7\frac{3}{32}}$	3 $b_{7\frac{7}{16}}$ 2 $d_{7\frac{1}{16}}$ 4 $d_{\frac{11}{16}} \times \frac{5}{32}$	7 $7\frac{7}{16}$ 2 $d_{7\frac{1}{4}}$	3 $b_{7\frac{1}{2}}$ 2 $d_{7\frac{1}{2}}$ 4 $d_{\frac{13}{32}} \times \frac{7}{16}$	Closed	Closed	9.5	31.5	33.8	88.8
7	Second set of duplex	3/4	0.1	8	1/8	$\frac{1}{8} \times 1\frac{1}{2}$	Closed	3 $b_{7\frac{3}{16}}$ 4 $d_{7\frac{3}{32}}$	3 Above block	7 Above block	3 Above block	Closed	Closed	9.5	31.5	33.8	81.5
7A	Second set of duplex	Plate re-moved	0.1	8	1/8	$\frac{1}{8} \times 1\frac{1}{2}$	Closed	3 $b_{7\frac{3}{16}}$ 4 $d_{7\frac{3}{32}}$	3 Above block	7 Above block	3 Above block	Closed	Closed	9.5	31.5	33.8	81.5
8	Second set of duplex	3/4	0.1	8	1/8	$\frac{1}{8} \times 1\frac{1}{2}$	$18 \times 10\frac{1}{2}$	3 $b_{7\frac{3}{16}}$ 4 $d_{7\frac{3}{32}}$	3 $b_{7\frac{7}{16}}$ 2 $d_{7\frac{1}{16}}$ 4 $d_{\frac{11}{16}} \times \frac{5}{32}$	7 $7\frac{7}{16}$ 2 $d_{7\frac{1}{4}}$	3 $b_{7\frac{3}{4}}$ 2 $d_{7\frac{1}{2}}$ 4 $d_{\frac{13}{32}} \times \frac{7}{16}$	Closed	Closed	9.5	31.5	39.0	91.0
9	Second set of duplex	3/4	0.1	8	1/8	$\frac{1}{8} \times 1\frac{1}{2}$	$18 \times 10\frac{1}{2}$	3 $b_{7\frac{3}{16}}$ 4 $d_{7\frac{3}{32}}$	3 Above block	7 $7\frac{7}{16}$ 2 $d_{7\frac{1}{4}}$	3 $b_{2.6\frac{5}{4}}$ 2 $d_{2.6\frac{1}{2}}$	Closed	Closed	10.0	31.5	15.8	70.7
9A	Second set of duplex	3/4	1.18	4	1/8	$\frac{1}{8} \times 1\frac{1}{2}$	$18 \times 10\frac{1}{2}$	3 $b_{7\frac{3}{16}}$ 4 $d_{7\frac{3}{32}}$	3 Above block	7 Above block	3 Above block	Closed	Closed	10.0	31.5	15.8	71.8
10	Second set of duplex	3/4	1.18	4	1/8	$\frac{1}{8} \times 1\frac{1}{2}$	$18 \times 10\frac{1}{2}$	3 $b_{7\frac{3}{16}}$ 4 $d_{7\frac{3}{32}}$	3 Above block	7 Above block	2 $d_{7\frac{1}{4}}$	Closed	Closed	10.0	31.5	10.3	84.4

11	Second set of duplex	3/4	1.16	4	1/8	$\frac{1}{8} \times 1 \frac{1}{2}$	$16 \times 10 \frac{1}{2}$	3 4	$b_{7 \frac{3}{16}} \frac{3}{4}$ $d_{7 \frac{3}{16}} \frac{3}{4}$	3 4	Above block	2	$o_{7 \frac{1}{16}} \frac{1}{16}$	2	$o_{7 \frac{1}{16}} \frac{1}{16}$	Closed	Closed	10.0	7.5	7.7	37.6
11B	Simplex	3/4	0.84	4	1/8	$\frac{1}{8} \times 1 \frac{1}{2}$	$16 \times 10 \frac{1}{2}$	3 4	$b_{7 \frac{3}{16}} \frac{3}{4}$ $d_{7 \frac{3}{16}} \frac{3}{4}$	3 4	Above block	2	$o_{7 \frac{1}{16}} \frac{1}{16}$	2	$o_{7 \frac{1}{16}} \frac{1}{16}$	Closed	Closed	10.0	7.5	7.7	34.3
12	Second set of duplex	3/4	0.84	4	1/8	$\frac{1}{8} \times 1 \frac{1}{2}$	$16 \times 10 \frac{1}{2}$	3 4	$b_{6 \frac{3}{16}} \frac{3}{4}$ $d_{6 \frac{3}{16}} \frac{3}{4}$	3 4	$b_{6 \frac{7}{16}} \frac{7}{16}$ $o_{7 \frac{1}{16}} \frac{1}{16}$ $d_{11 \frac{5}{16}} \frac{5}{16}$	2 7	$o_{7 \frac{1}{16}} \frac{1}{16}$ $b_{1 \frac{1}{2}} \frac{1}{2}$	2 5	$o_{7 \frac{1}{16}} \frac{1}{16}$	Closed	Closed	9.5	28.5	16.7	67.4
13	Second set of duplex	3/4	0.84	4	1/8	$\frac{1}{8} \times 1 \frac{1}{2}$	$16 \times 10 \frac{1}{2}$	3 4	$b_{6 \frac{3}{16}} \frac{3}{4}$ $d_{6 \frac{3}{16}} \frac{3}{4}$	3 4	Above block	2 7	Above block	2 5	Above block	Closed	Closed	10.5	28.5	16.7	67.8
13B	Third set of duplex	1.0	0.84	4	1/8	$\frac{1}{8} \times 1 \frac{1}{2}$	$16 \times 10 \frac{1}{2}$	3 4	$b_{6 \frac{3}{16}} \frac{3}{4}$ $d_{6 \frac{3}{16}} \frac{3}{4}$	3 4	Above block	2 7	Above block	2 5	Above block	Closed	Closed	10.5	28.5	16.7	67.9
14	Third set of duplex	1.0	0.84	4	1/8	$\frac{1}{8} \times 1 \frac{1}{2}$	$16 \times 10 \frac{1}{2}$	3 4	$b_{6 \frac{3}{16}} \frac{3}{4}$ $d_{6 \frac{3}{16}} \frac{3}{4}$	3 4	Above block	2 7	Above block	2 2	$o_{7 \frac{1}{16}} \frac{1}{16}$ $b_{1 \frac{1}{2}} \frac{1}{2}$	Closed	Closed	10.5	28.5	13.7	64.0
15	Third set of duplex	1.0	0.84	4	1/8	$\frac{1}{8} \times 1 \frac{1}{2}$	$16 \times 10 \frac{1}{2}$	3 4	$b_{6 \frac{3}{16}} \frac{3}{4}$ $d_{6 \frac{3}{16}} \frac{3}{4}$	3 4	Above block	2 7	Above block	2 2	Above block	Closed	Closed	10.5	28.5	16.7	67.0
16	Fourth set of duplex and new semi-fold	1.0	0.64	4	1/8	$\frac{1}{8} \times 1 \frac{1}{2}$	$16 \times 10 \frac{1}{2}$	3 4	$b_{6 \frac{3}{16}} \frac{3}{4}$ $d_{6 \frac{3}{16}} \frac{3}{4}$	3 4	Above block	2 7	$b_{7 \frac{1}{16}} \frac{1}{16}$ $b_{2 \frac{3}{4}} \frac{3}{4}$	2 5	$o_{7 \frac{1}{16}} \frac{1}{16}$	Closed	Closed	10.5	18.0	19.2	32.4
17	Fourth set of duplex and new semi-fold	1.0	0.64	4	1/8	$\frac{1}{8} \times 1 \frac{1}{2}$	$16 \times 10 \frac{1}{2}$	3 4	$b_{6 \frac{3}{16}} \frac{3}{4}$ $d_{6 \frac{3}{16}} \frac{3}{4}$	3 4	Above block	2 7	Above block	2	$o_{7 \frac{1}{16}} \frac{1}{16}$	Closed	Closed	10.5	18.0	7.7	48.0
18	Fourth set of duplex and new semi-fold	1.0	0.64	4	1/8	Closed	Closed	3 4	$b_{6 \frac{3}{16}} \frac{3}{4}$ $d_{6 \frac{3}{16}} \frac{3}{4}$	3 4	Above block	2 7	Above block	2	$o_{7 \frac{1}{16}} \frac{1}{16}$	Closed	4x9.5	10.5	18.0	7.7	43.5
19	Fourth set of duplex and new semi-fold	1.0	0.84	4	1/8	Closed	Closed	3 4	$b_{6 \frac{3}{16}} \frac{3}{4}$ $d_{6 \frac{3}{16}} \frac{3}{4}$	1 4	$b_{6 \frac{7}{16}} \frac{7}{16}$ $o_{7 \frac{1}{16}} \frac{1}{16}$ $d_{11 \frac{5}{16}} \frac{5}{16}$	2 7	$o_{7 \frac{1}{16}} \frac{1}{16}$ $b_{2 \frac{3}{4}} \frac{3}{4}$	2	$o_{7 \frac{1}{16}} \frac{1}{16}$	Closed	4x9.5	10.5	18.0	4.7	40.7
20	Fourth set of duplex and new semi-fold	1.0	0.1	8	1/8	Closed	Closed	3 4	$b_{6 \frac{3}{16}} \frac{3}{4}$ $d_{6 \frac{3}{16}} \frac{3}{4}$	3 4	$b_{6 \frac{7}{16}} \frac{7}{16}$ $o_{7 \frac{1}{16}} \frac{1}{16}$ $d_{11 \frac{5}{16}} \frac{5}{16}$	2 7	$o_{7 \frac{1}{16}} \frac{1}{16}$ $b_{2 \frac{3}{4}} \frac{3}{4}$	2	$o_{7 \frac{1}{16}} \frac{1}{16}$	16×20	16×9.5	10.5	10.0	5.4	41.4

^aSlots located at center and $11 \frac{1}{4} \frac{1}{2}$, $26 \frac{1}{2} \frac{1}{2}$, and $35 \frac{3}{4} \frac{3}{4}$ to right and left on combustor liner outer wall; slots at center and $26 \frac{1}{2} \frac{1}{2}$ to right and left on combustor liner inner wall (unless otherwise noted) (see fig. 23).

^bSlots at center and $26 \frac{1}{2} \frac{1}{2}$ to right and left.

^cDenotes wall clearance.

^dSlots at $11 \frac{1}{4} \frac{1}{2}$ and $35 \frac{3}{4} \frac{3}{4}$ to right and left.

^eSlots at center and $26 \frac{1}{2} \frac{1}{2}$ to left.

^fSlot at center.

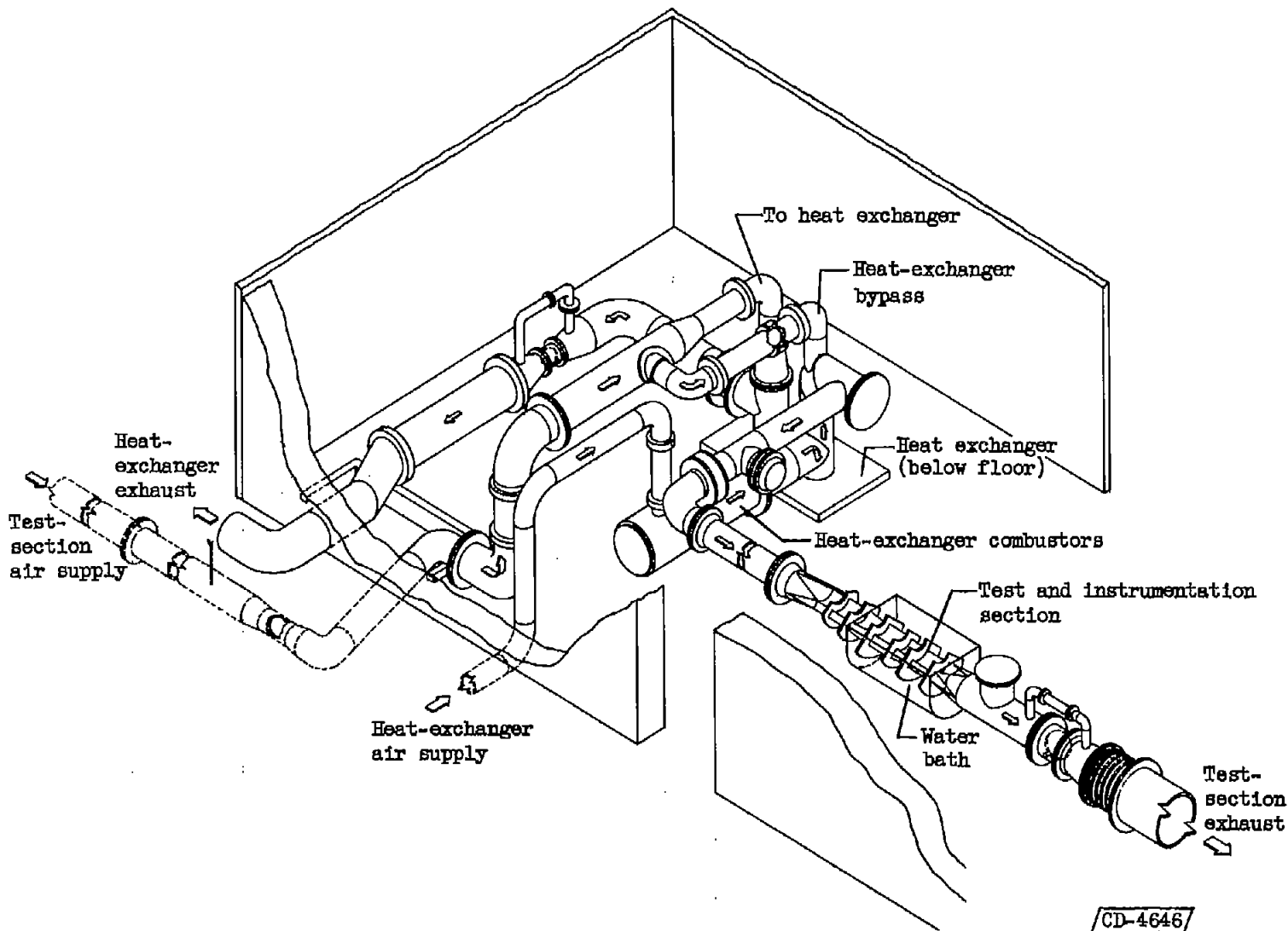


Figure 1. - Sketch of test installation.

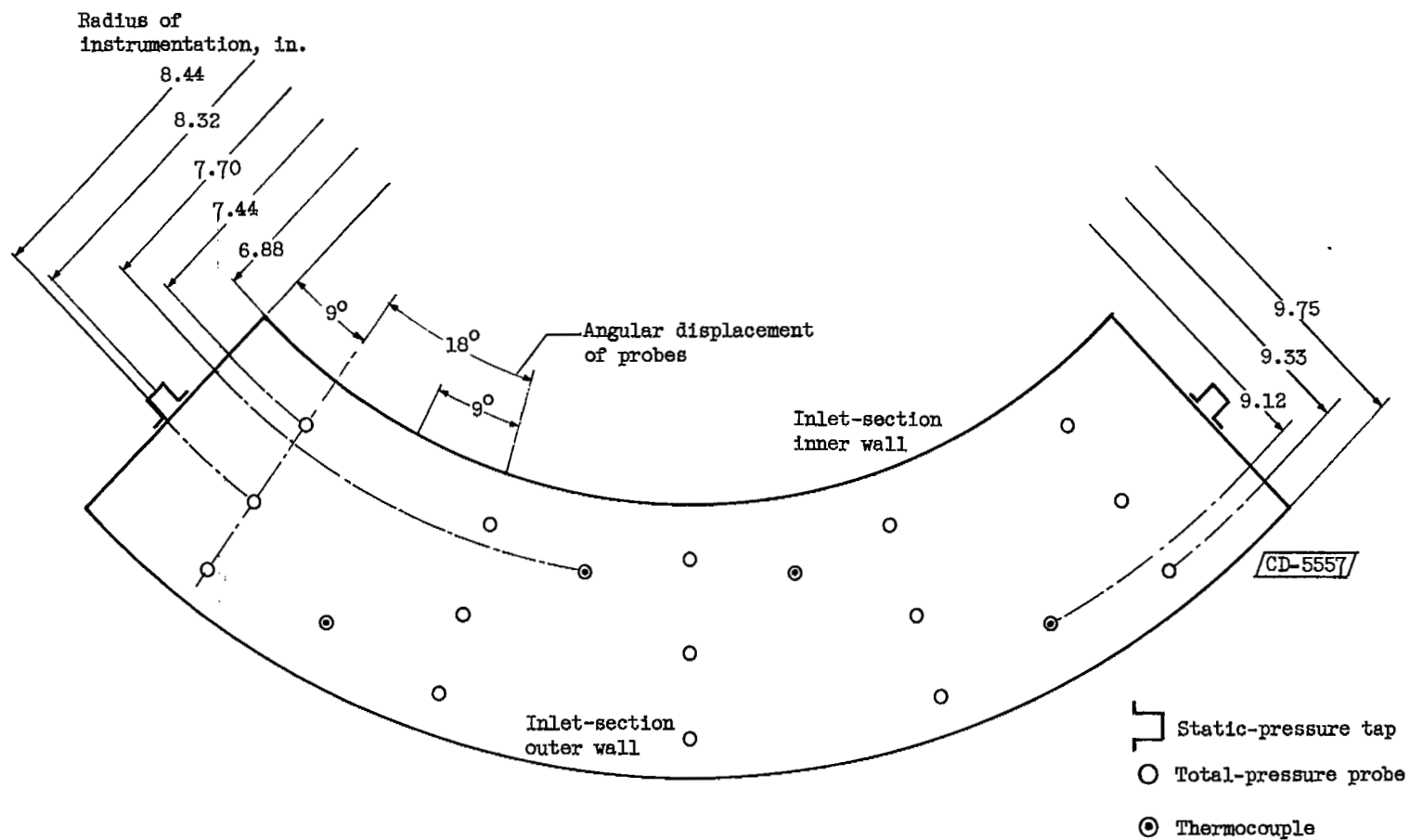


Figure 3. - Cross section of inlet-air instrumentation section (station 1, fig. 2) showing location of temperature- and pressure-measuring probes at centers of equal areas and static pressure taps.

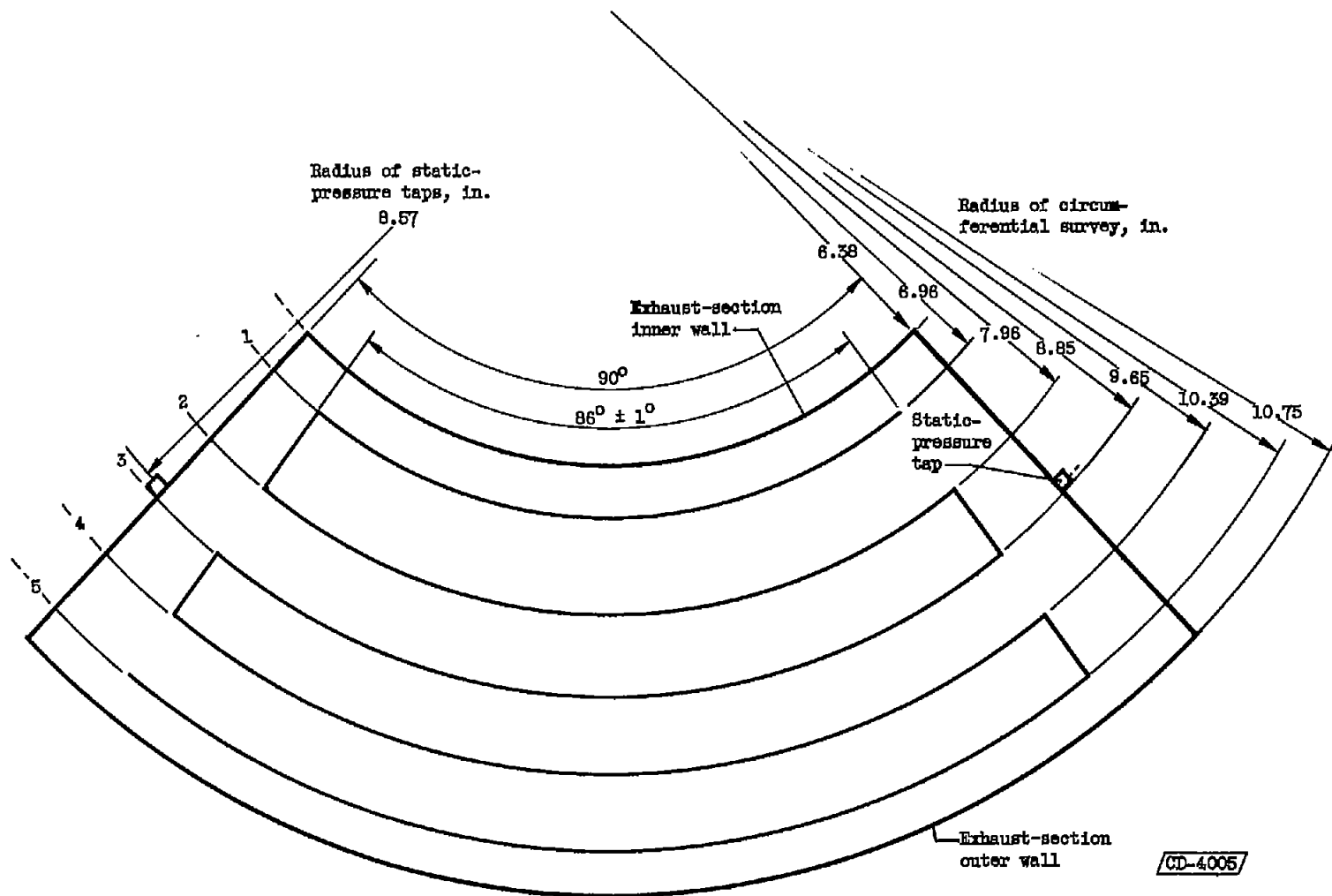


Figure 4. - Paths of probe tips of polar-coordinate survey system across combustor outlet section (station 2, fig. 2), showing circumferential sweeps at five radii at centers of equal areas for measuring temperatures and total pressures.

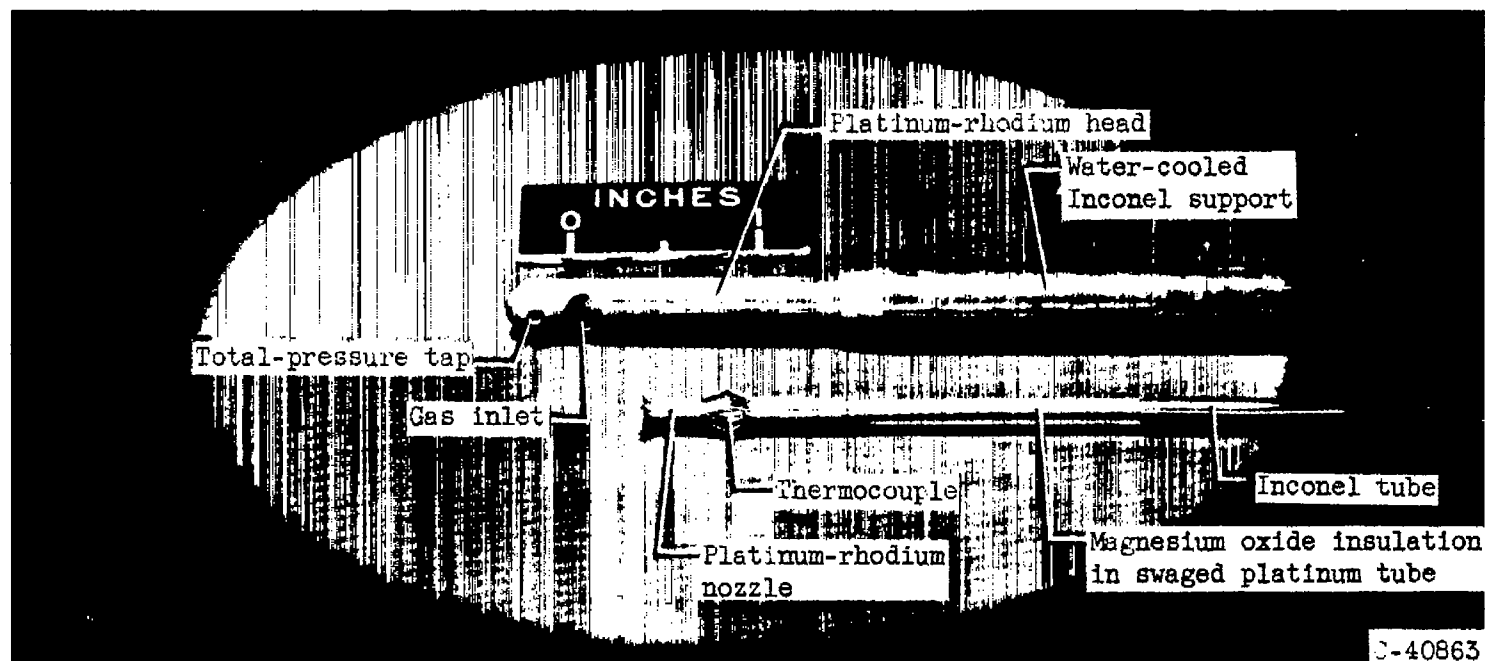


Figure 5. - Probe sensing-head detail.

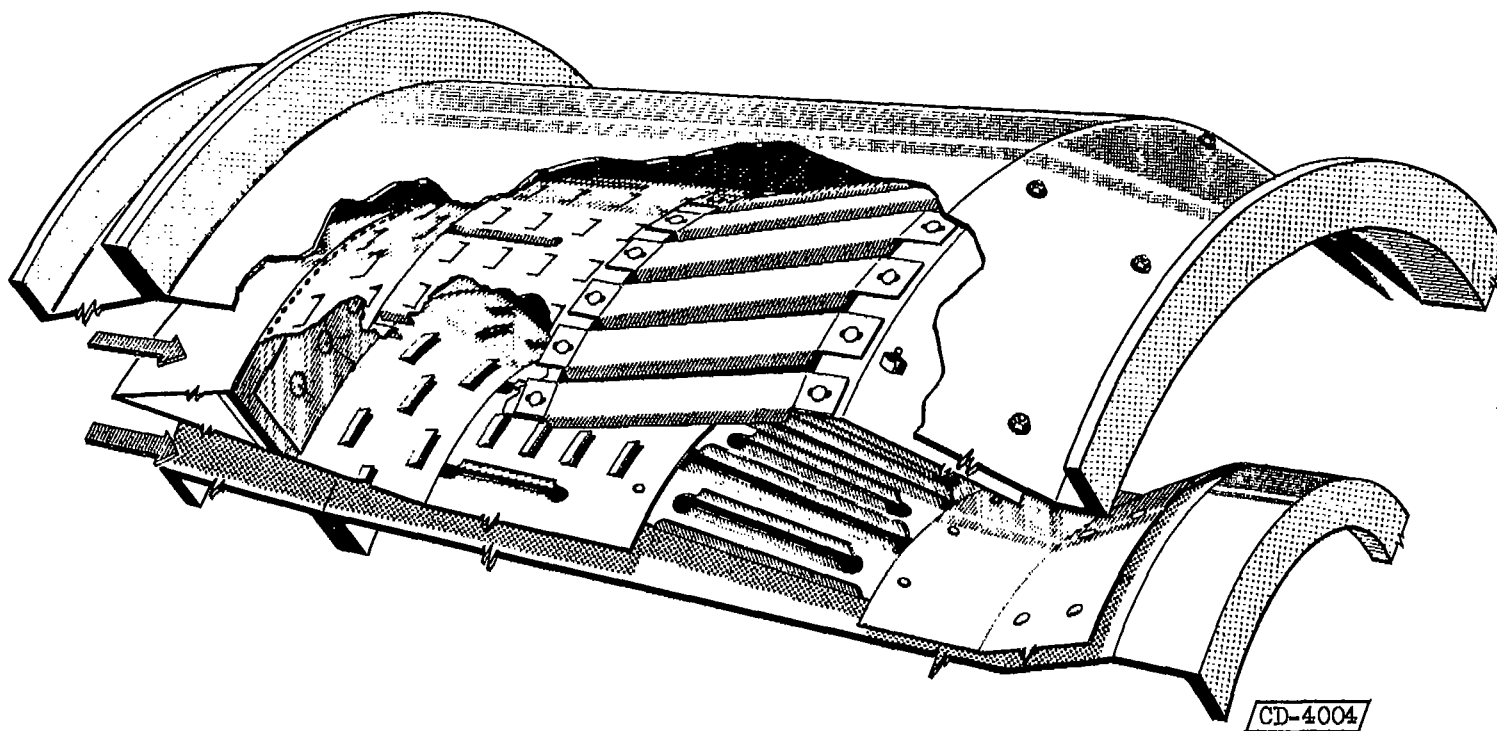


Figure 6. - Three-quarter-cutaway view of design I experimental channeled-wall annular combustor assembled in housing.

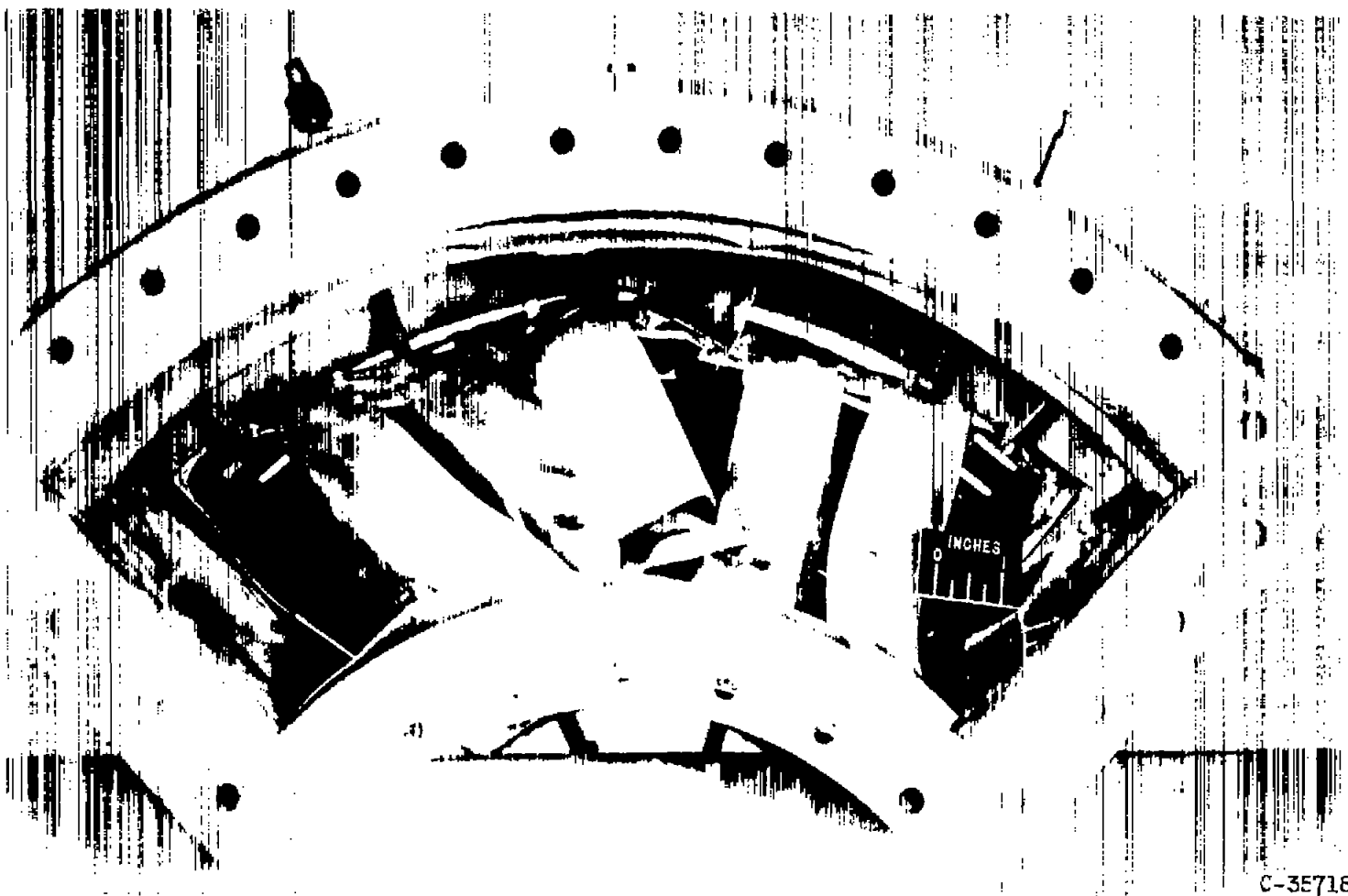
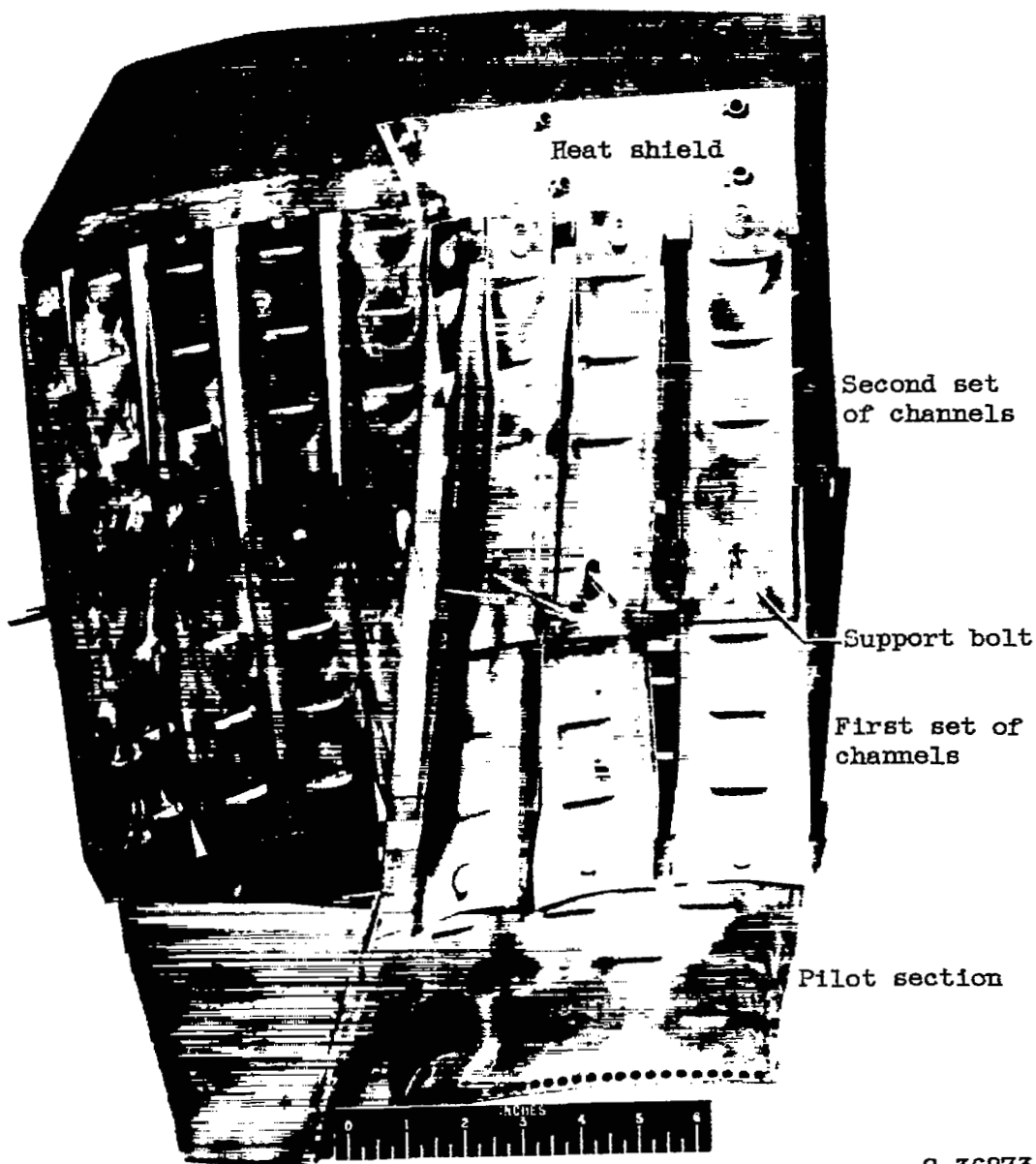


Figure 7. - Design I combustor after 1 hour of operation at condition C-2 with an average exhaust temperature of about 2100° F.

4378



C-36873

Figure 8. - Design I configuration with two sets of channel sections.

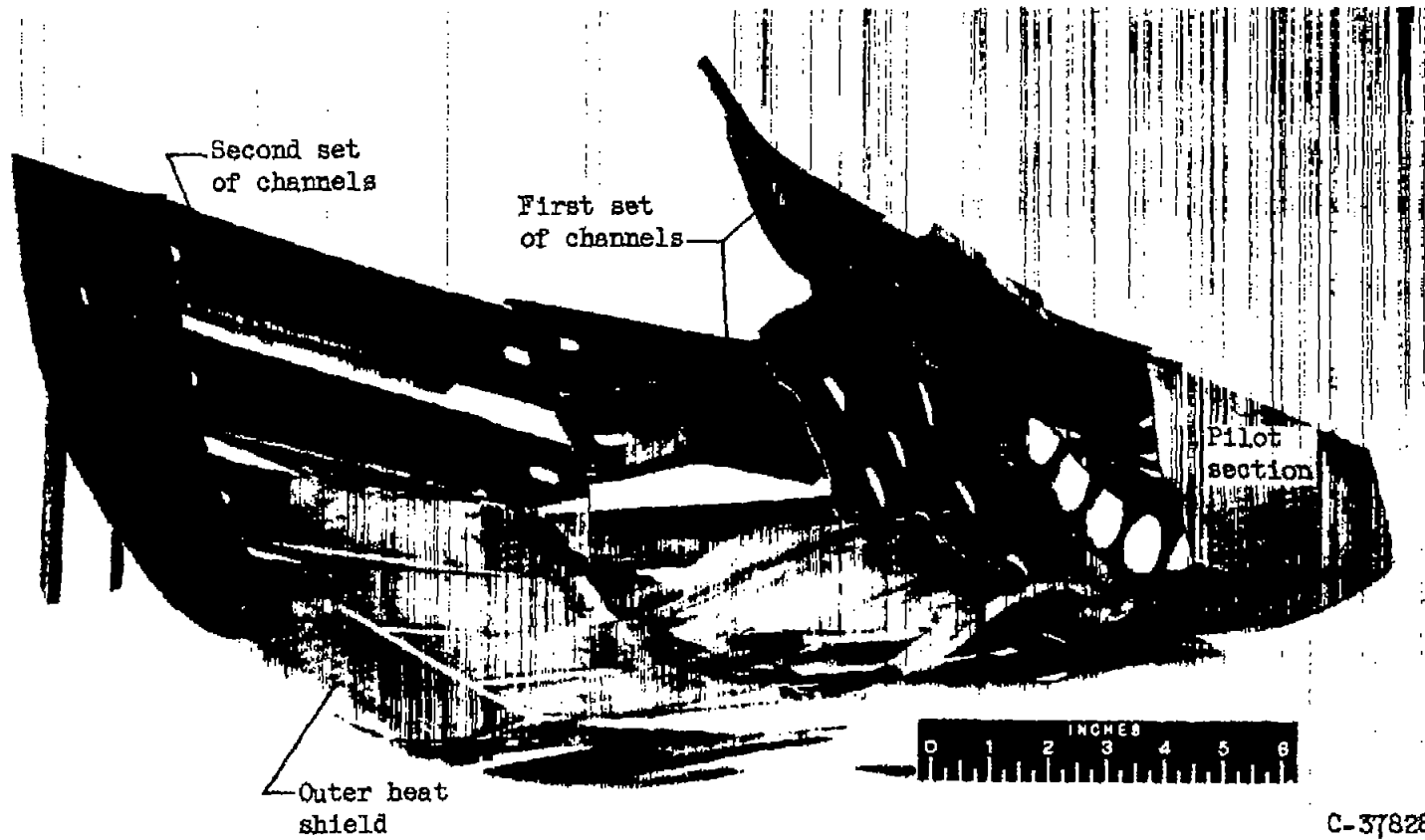
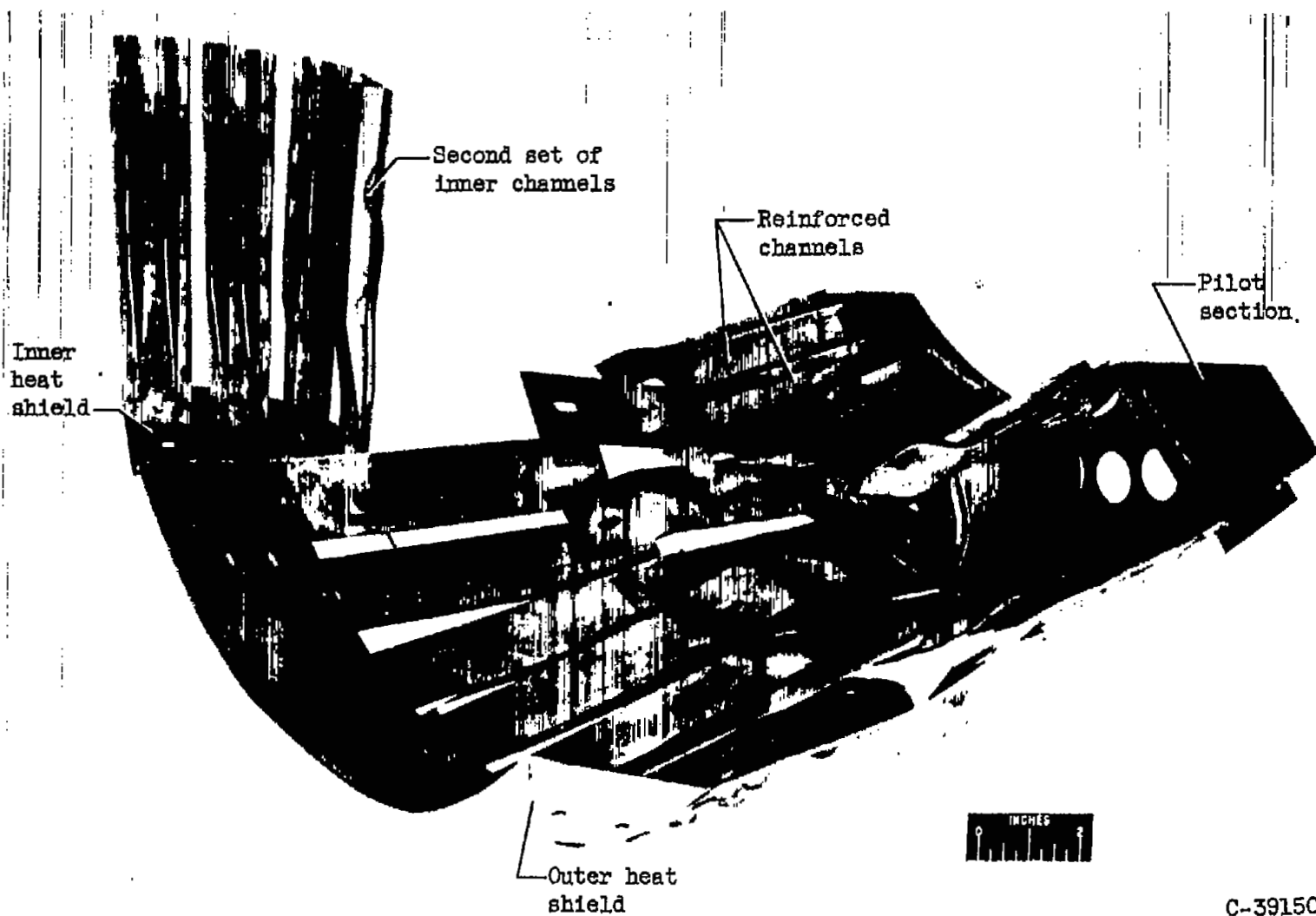
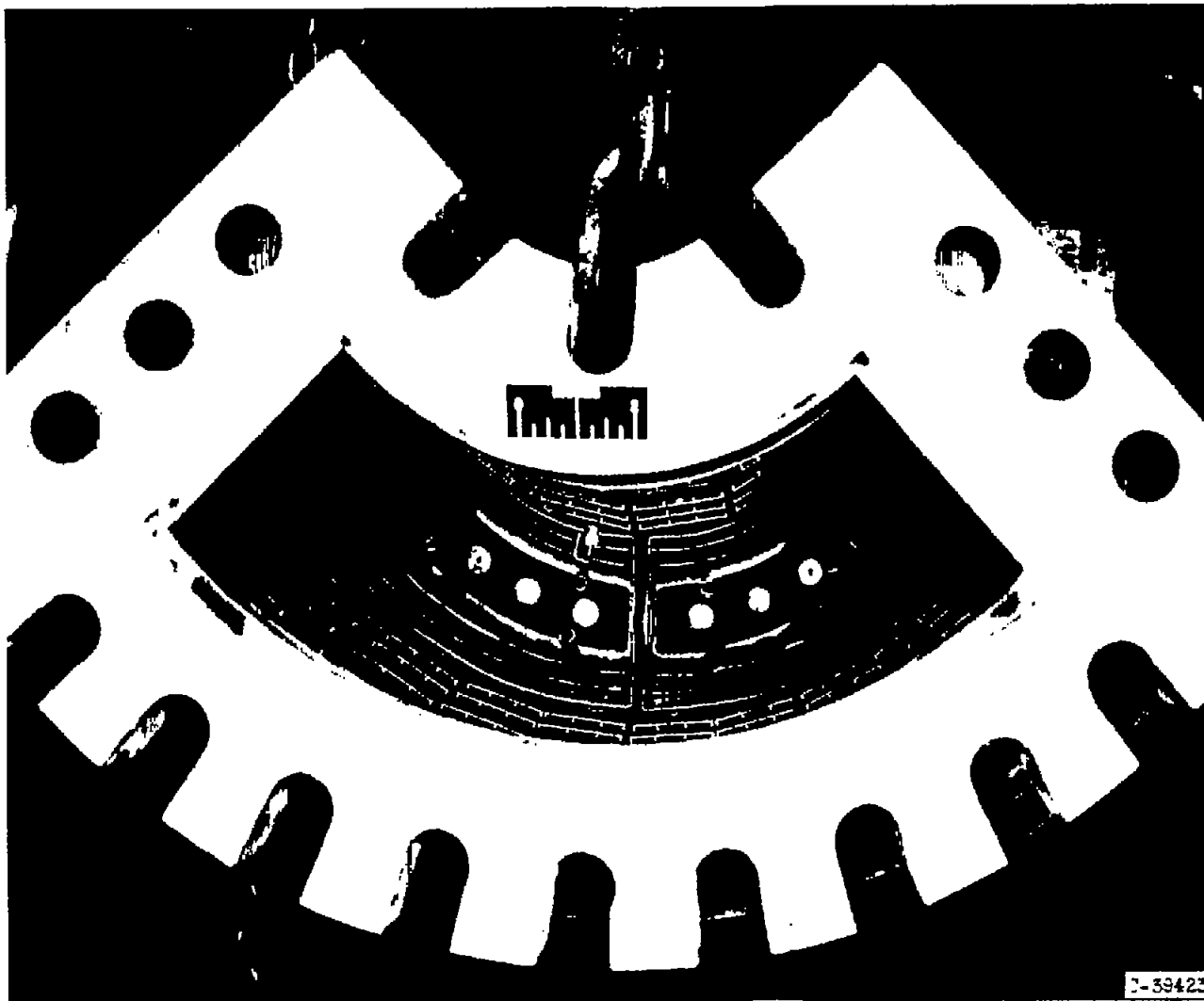


Figure 9. - Design I configuration with 1/16-inch metal thickness after 2 hours of run time.



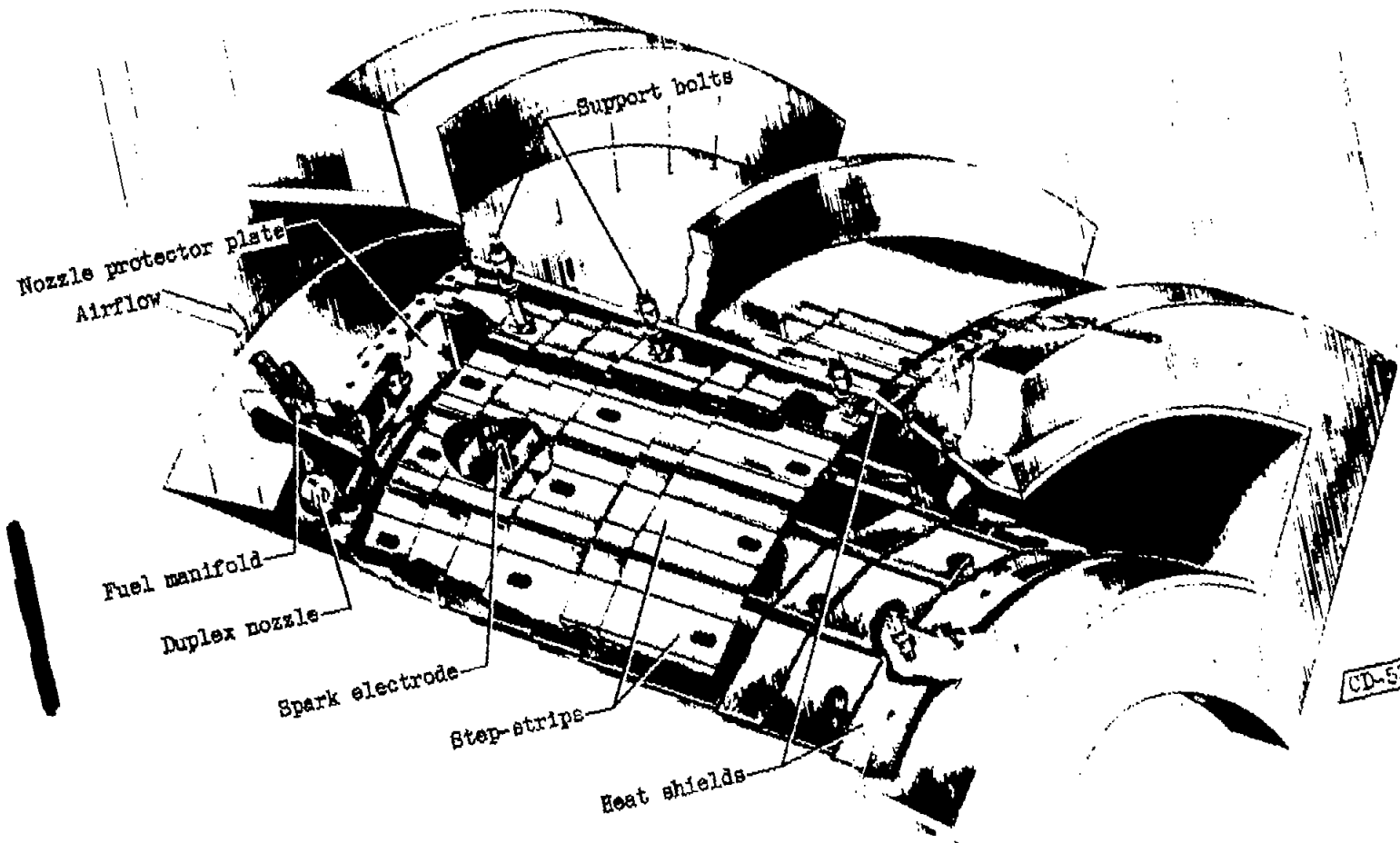
C-39150

Figure 10. - Design I configuration with split pilot sections and reinforced channels after 2 hours of run time.



(a) Photograph of configuration 1 installed in housing, after 11 hours of run time.

Figure 11. - Design II combustor.



CD-5355

(b) Cutaway drawing.

Figure 11. - Concluded. Design II combustor.

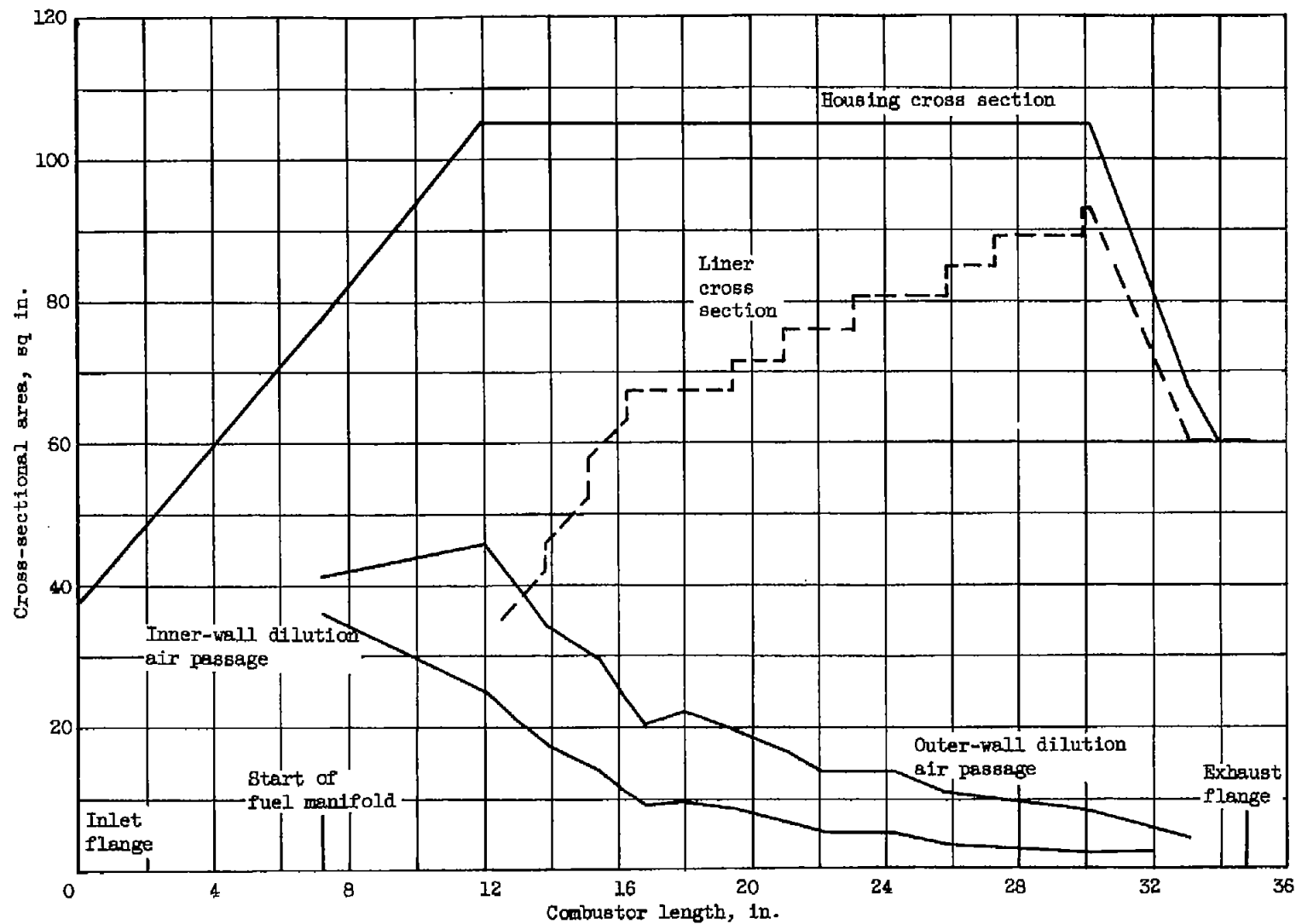


Figure 12. - Combustor length against cross-sectional area of housing, flame zone, and inner- and outer-wall dilution air passages for design II combustors.

4378

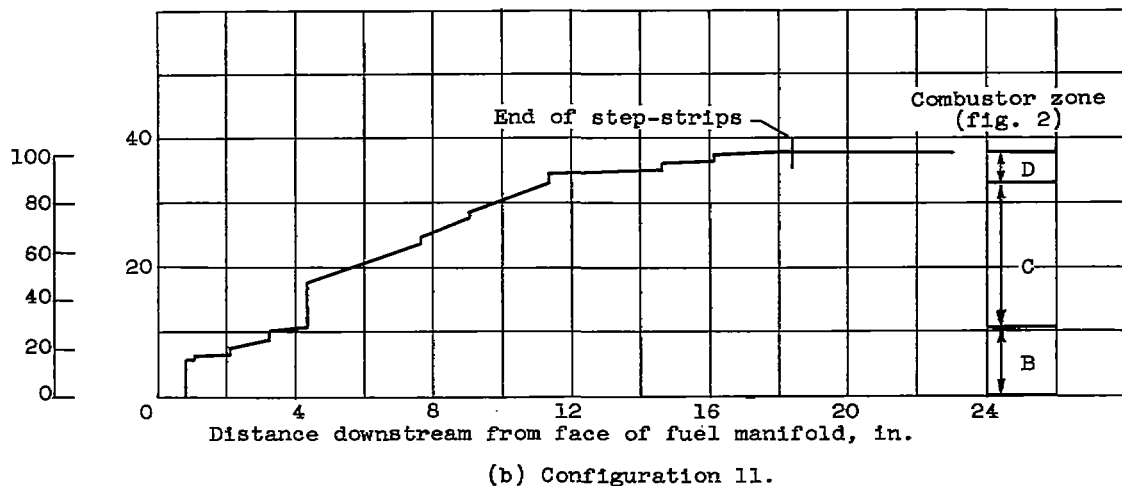
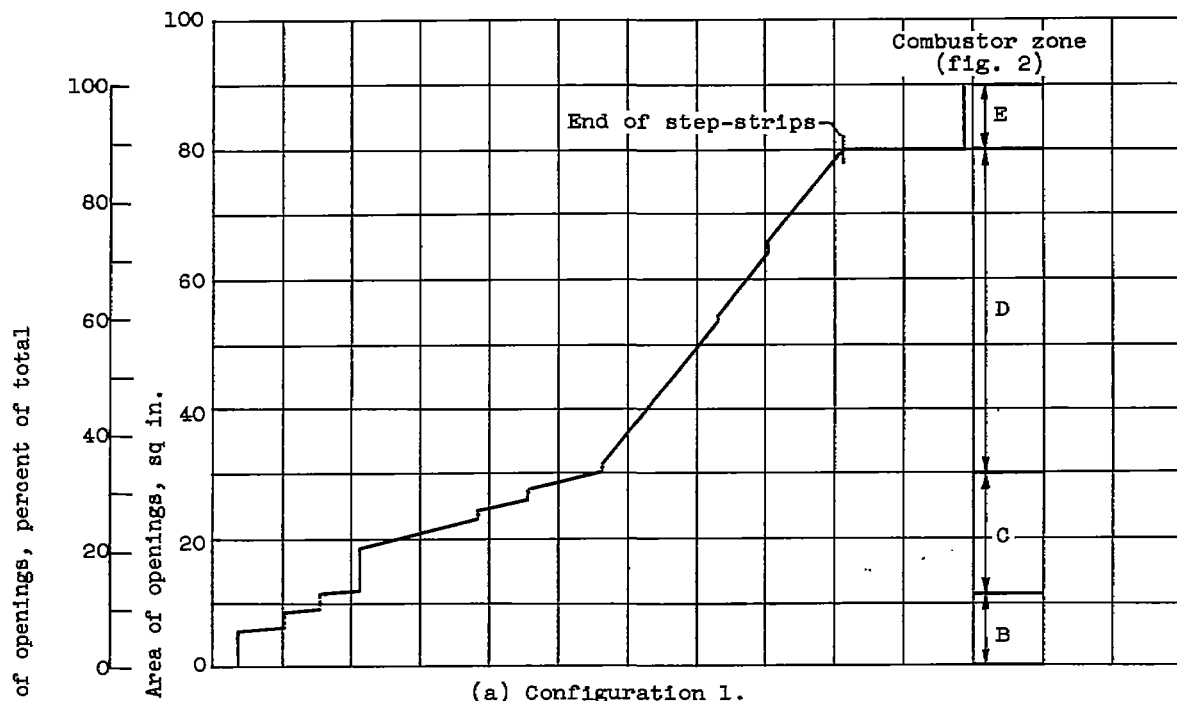


Figure 13. - Variation in air-admission hole area with distance downstream from face of fuel manifold for four design II configurations.

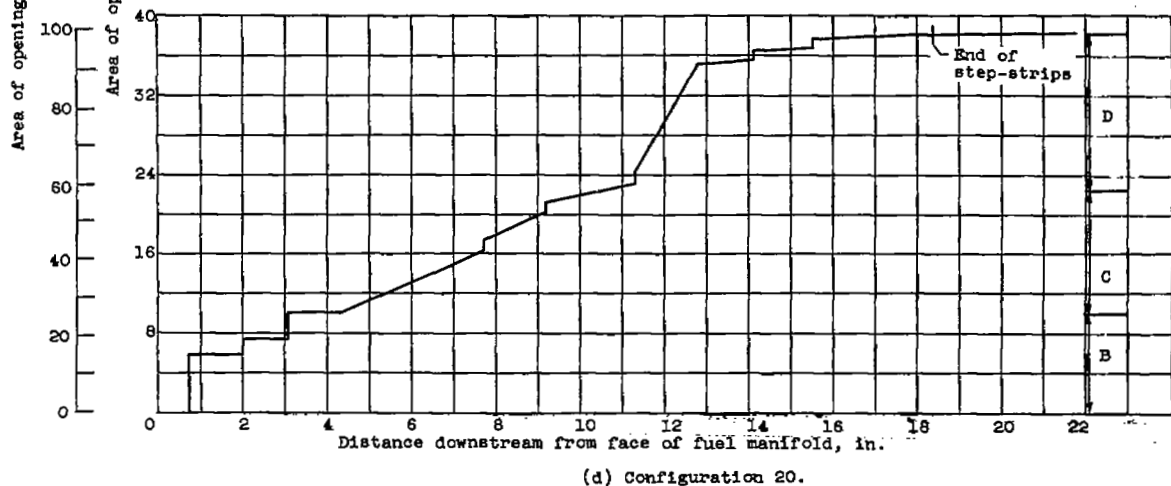
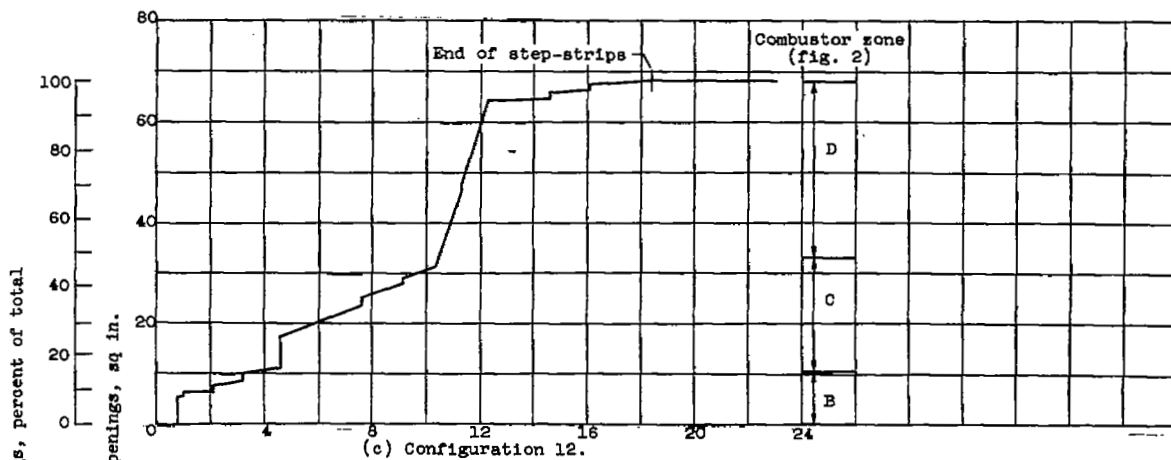


Figure 13. - Concluded. Variation in air-admission hole area with distance downstream from face of fuel manifold for four design II configurations.

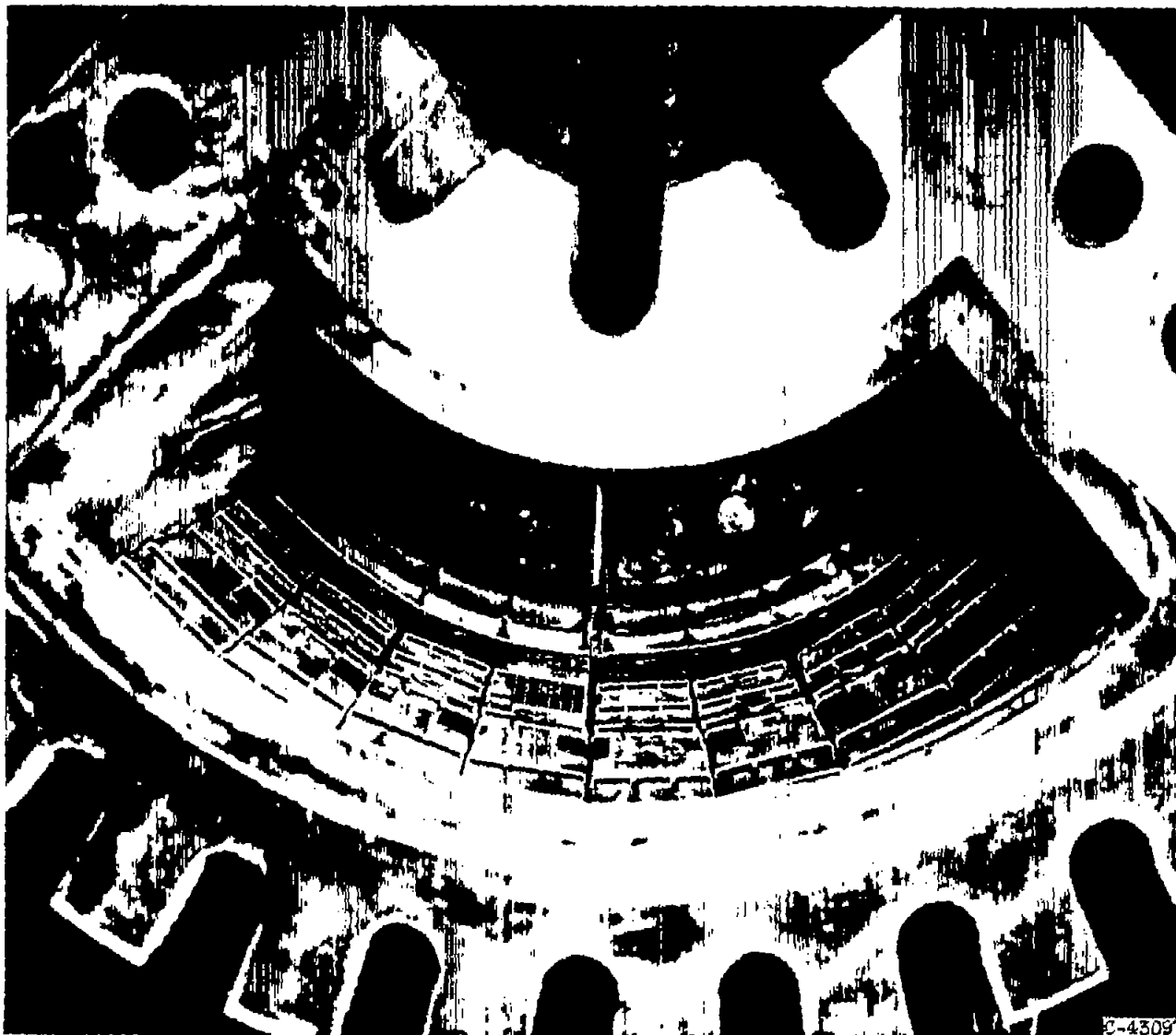


Figure 14. - Configuration 20 installed in housing, after about 40 hours of run time.
(Total run time with all configurations was about 150 hours.)

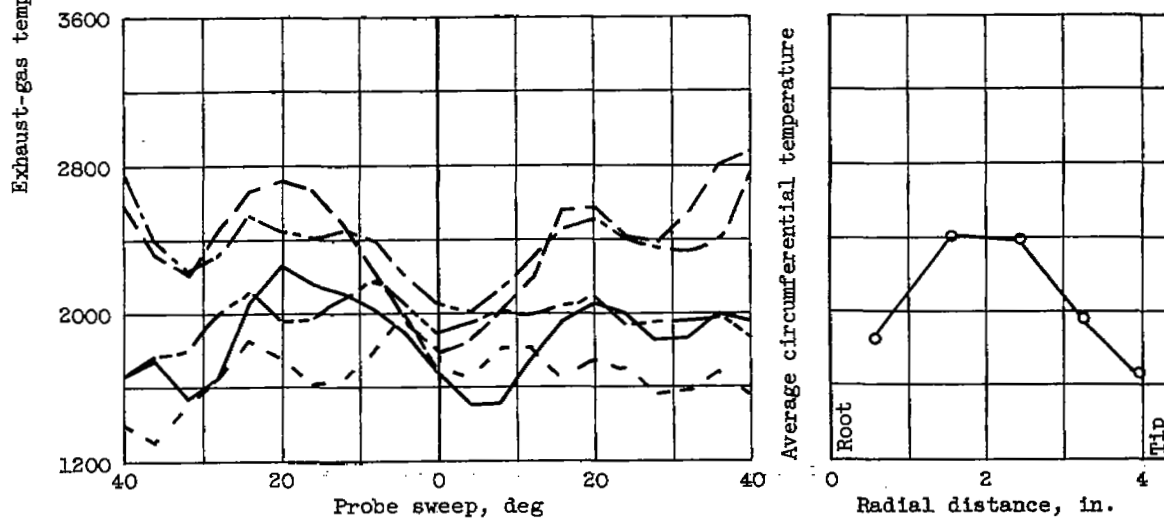
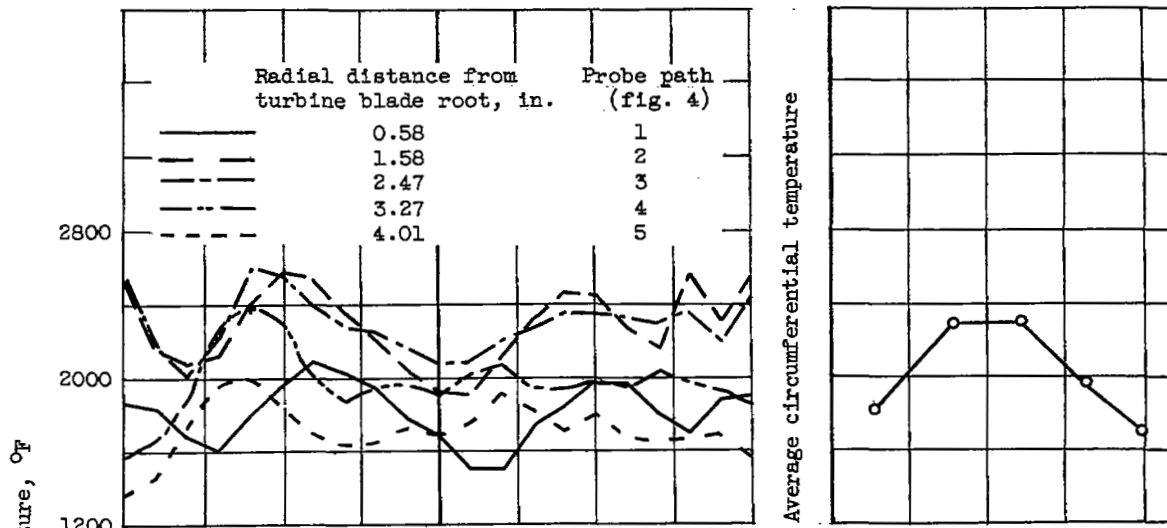


Figure 15. - Exhaust-gas temperature patterns for configuration 20 at start and end of run at condition D.

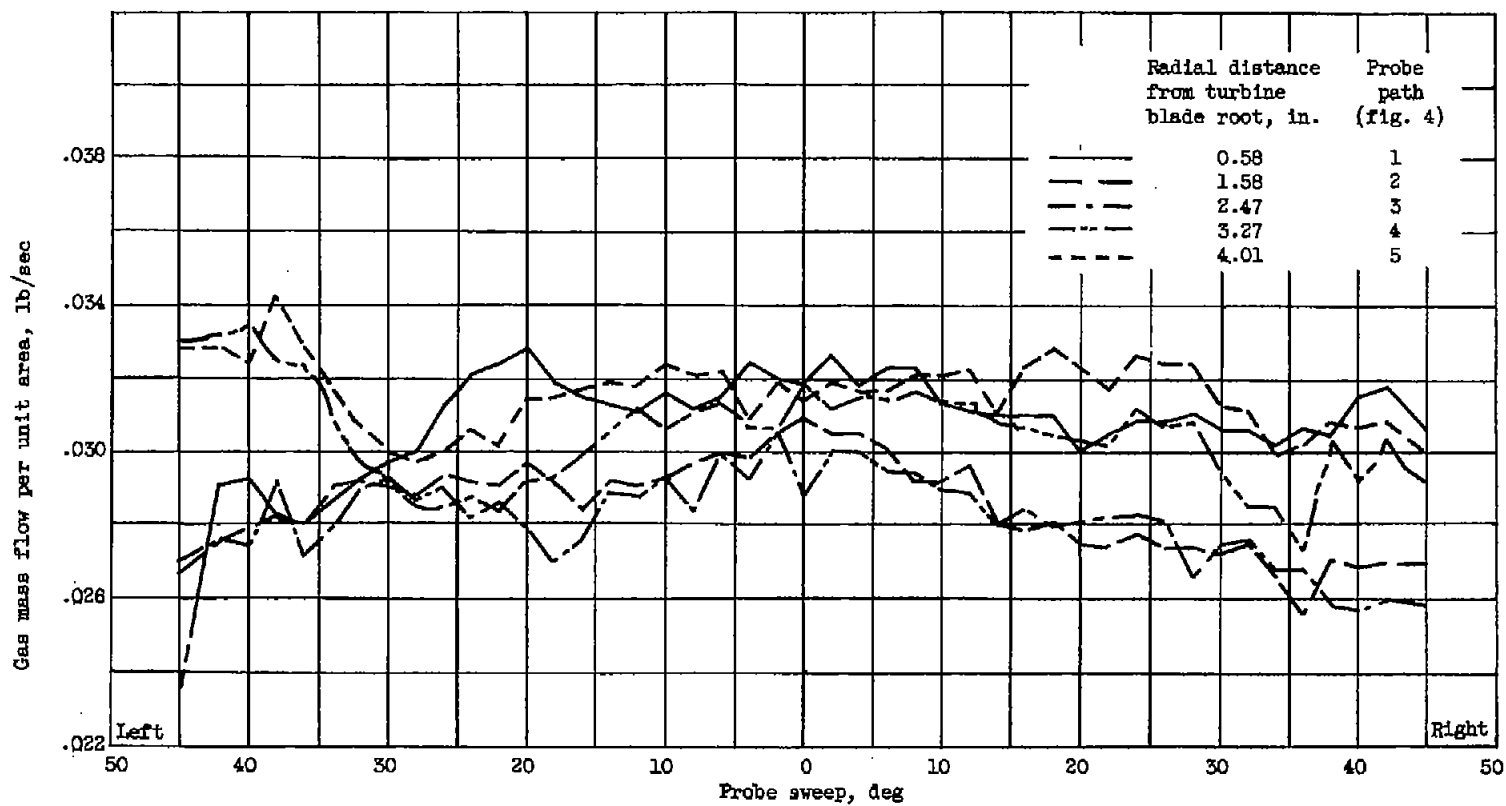


Figure 17. - Variation in gas mass flow across exhaust duct for a representative run.

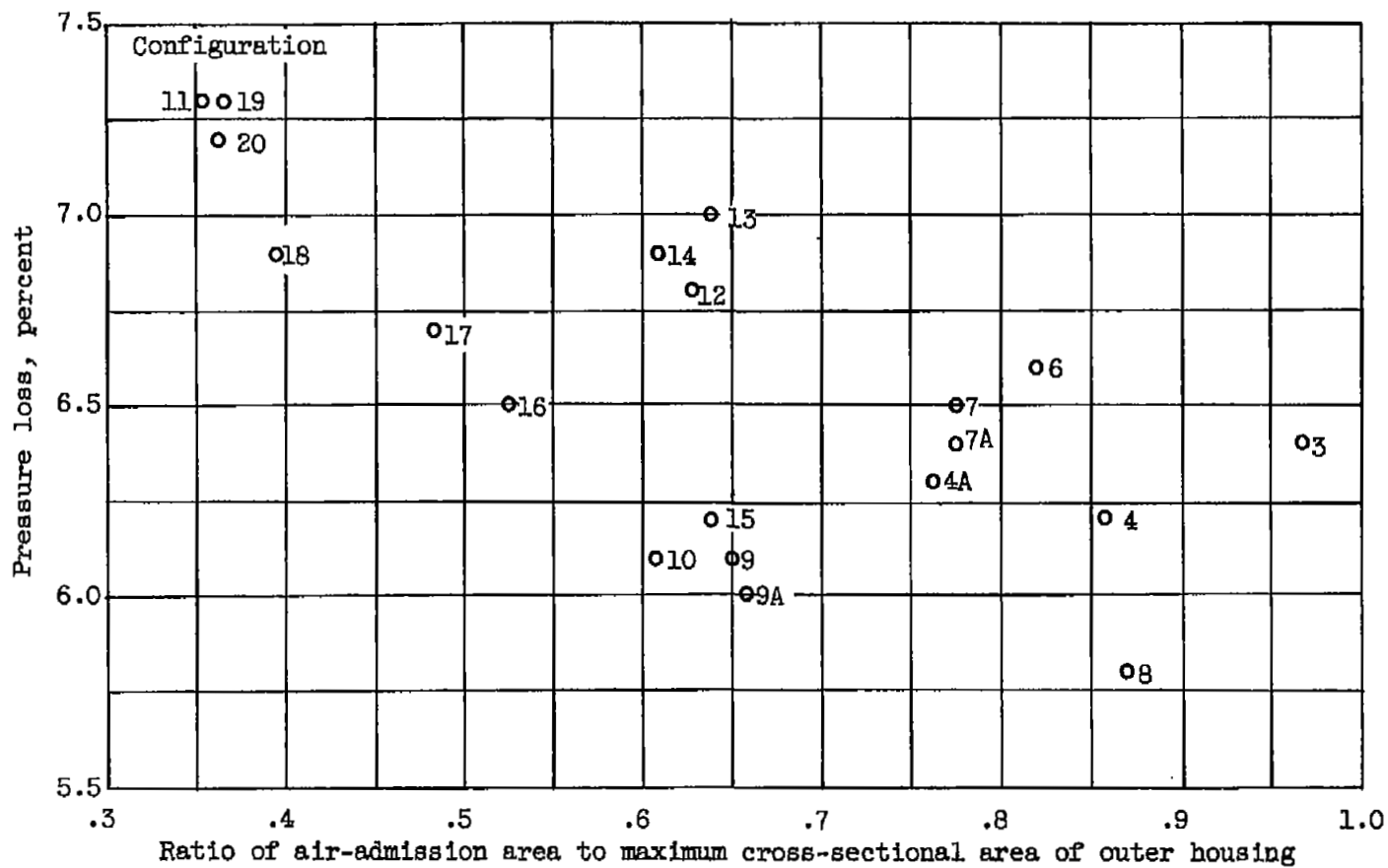


Figure 18. - Variation in pressure loss with ratio of air-admission area to reference area for design II configurations. Test condition B; average exhaust-gas temperatures, 1700° to 2100° F.

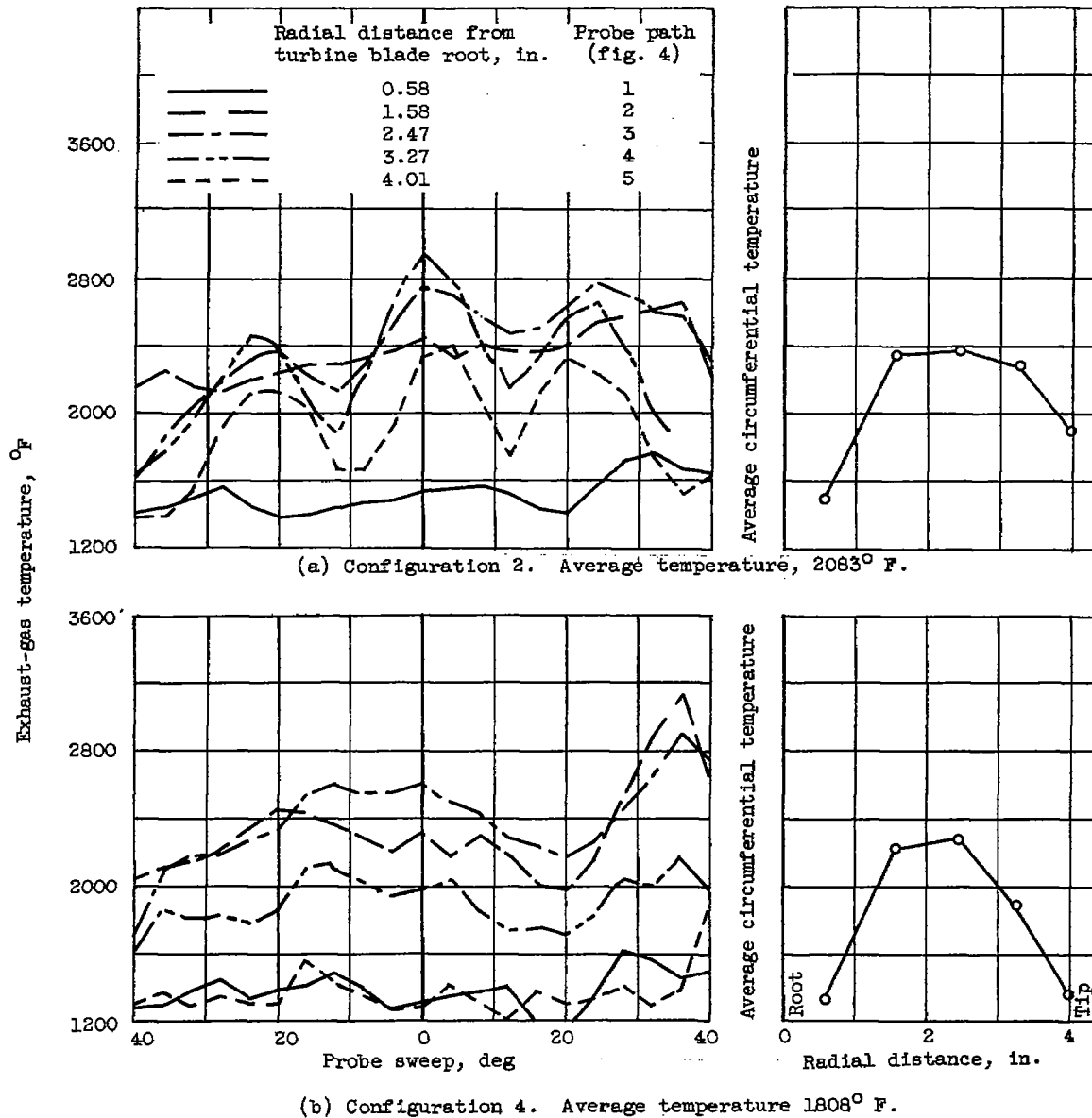
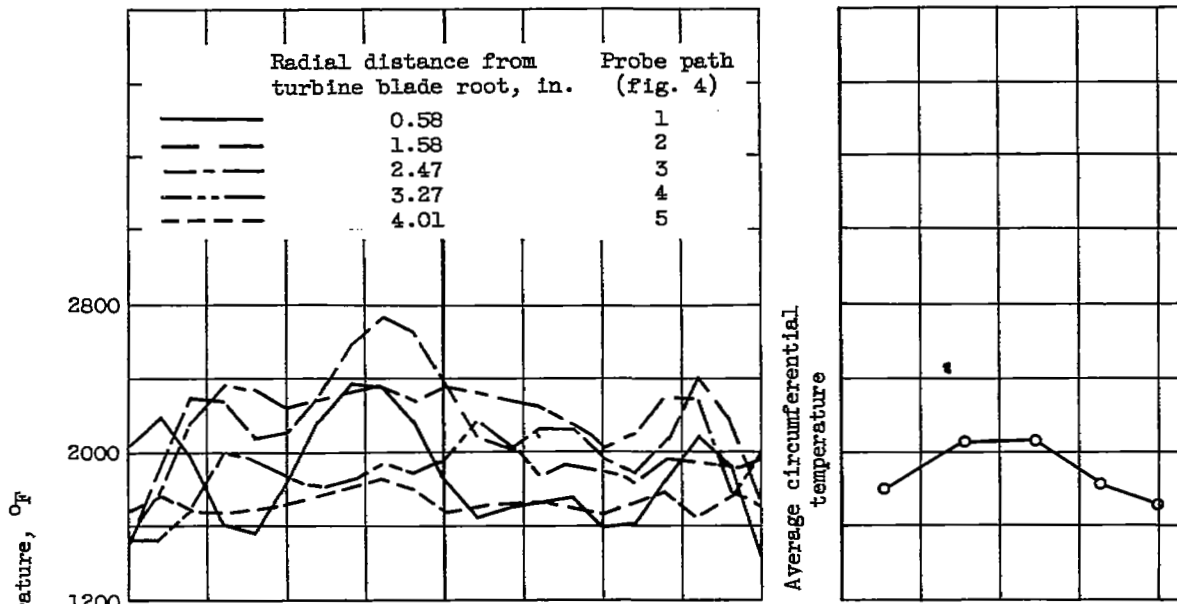
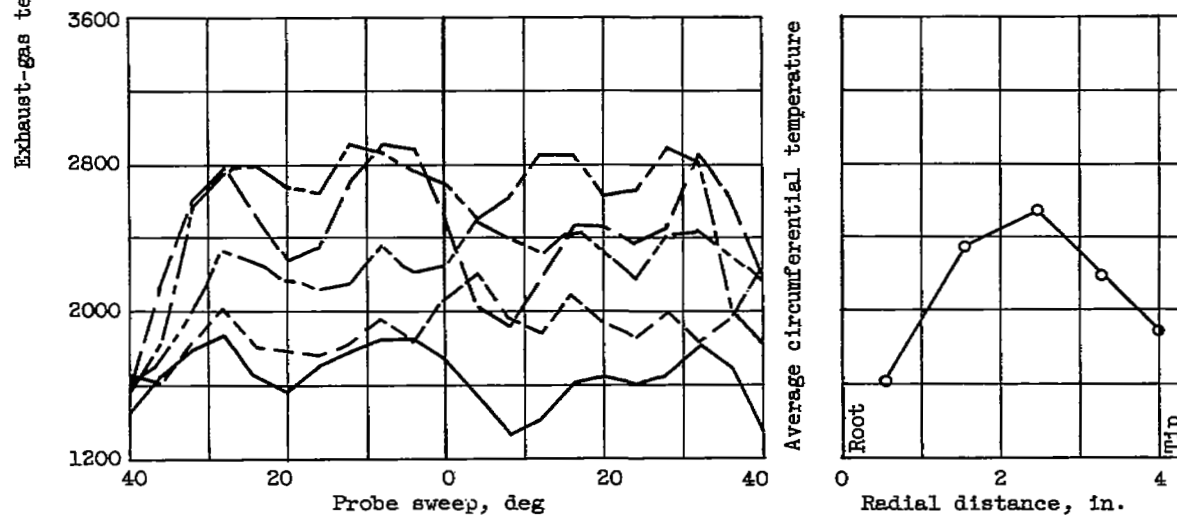


Figure 19. - Exhaust-gas temperature patterns for selected design II configurations. Test condition B.

4378

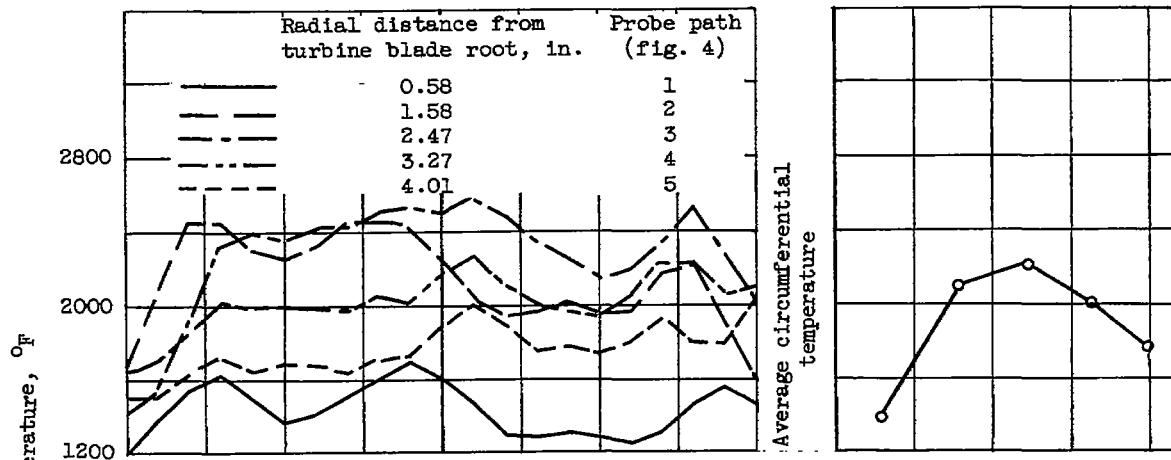


(c) Configuration 4A. Average temperature, 1890° F.

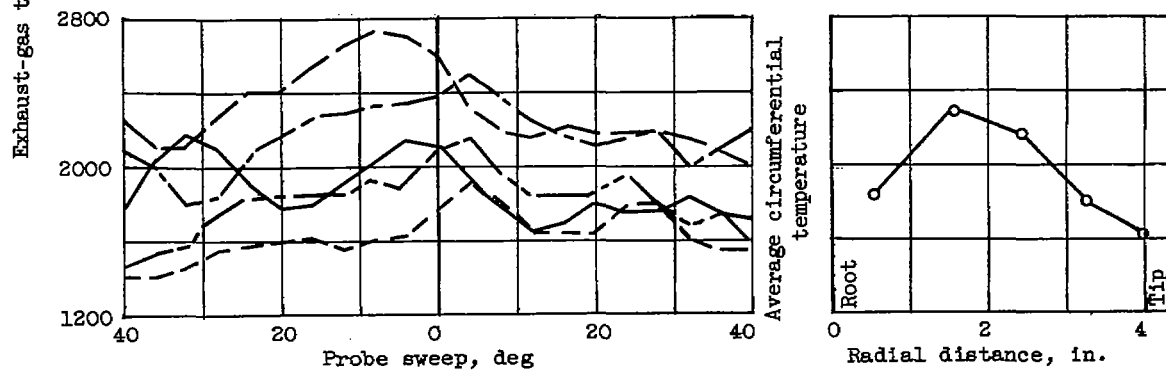


(d) Configuration 6. Average temperature, 2099° F.

Figure 19. - Continued. Exhaust-gas temperature patterns for selected design II configurations. Test condition B.



(e) Configuration 8. Average temperature, 1900° F.



(f) Configuration 9. Average temperature, 1944° F.

Figure 19. - Continued. Exhaust-gas temperature patterns for selected design II configurations. Test condition B.

4378

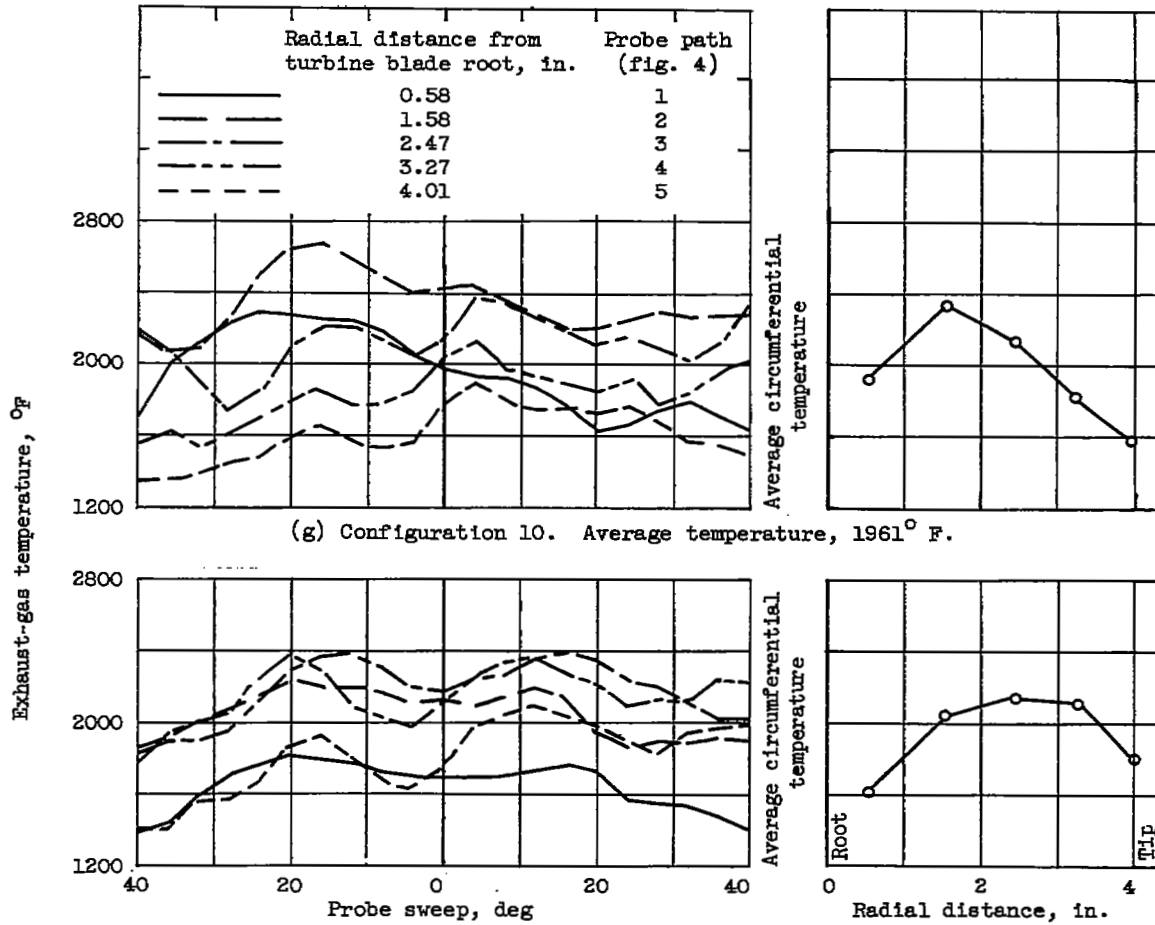


Figure 19. - Concluded. Exhaust-gas temperature patterns for selected design II configurations. Test condition B.

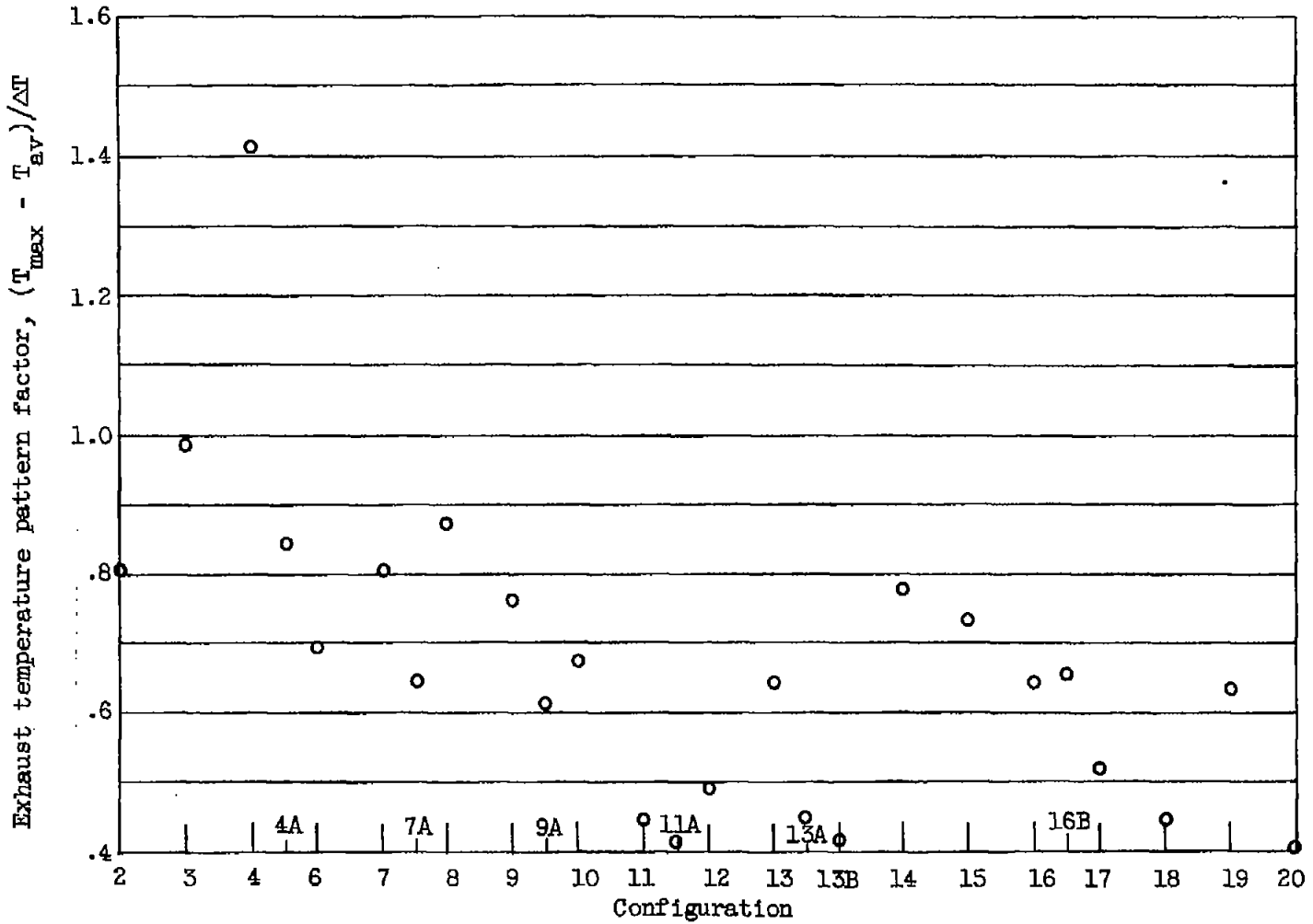


Figure 20. - Exhaust temperature pattern factor for design II configurations with fuel injected through small-slot systems of nozzles. Test condition B; average temperatures, 1800° to 2150° F.

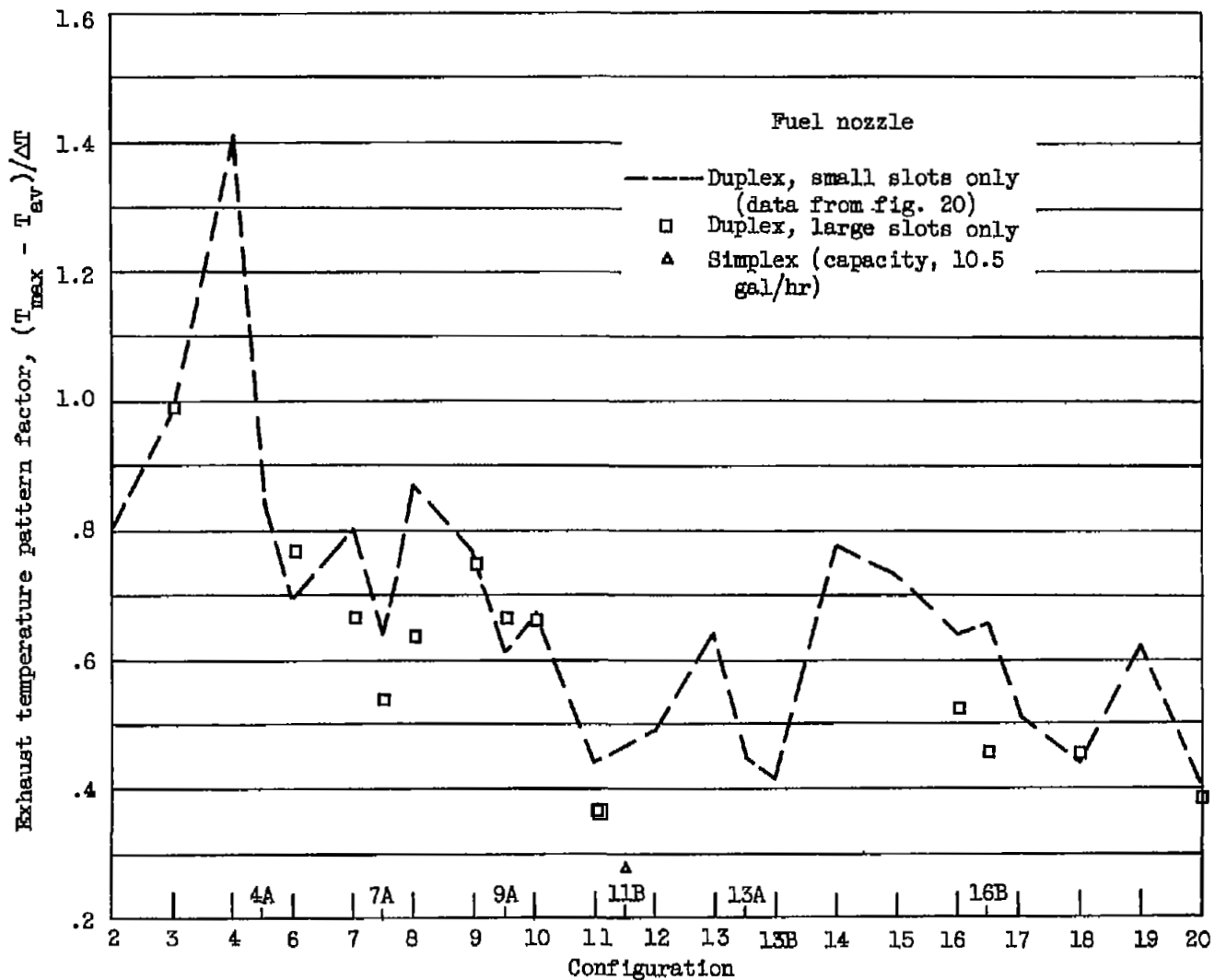


Figure 21. - Exhaust temperature pattern factor for design II configurations operating with different fuel-injector systems. Test condition B; average temperatures, 1800° to 2150° F.

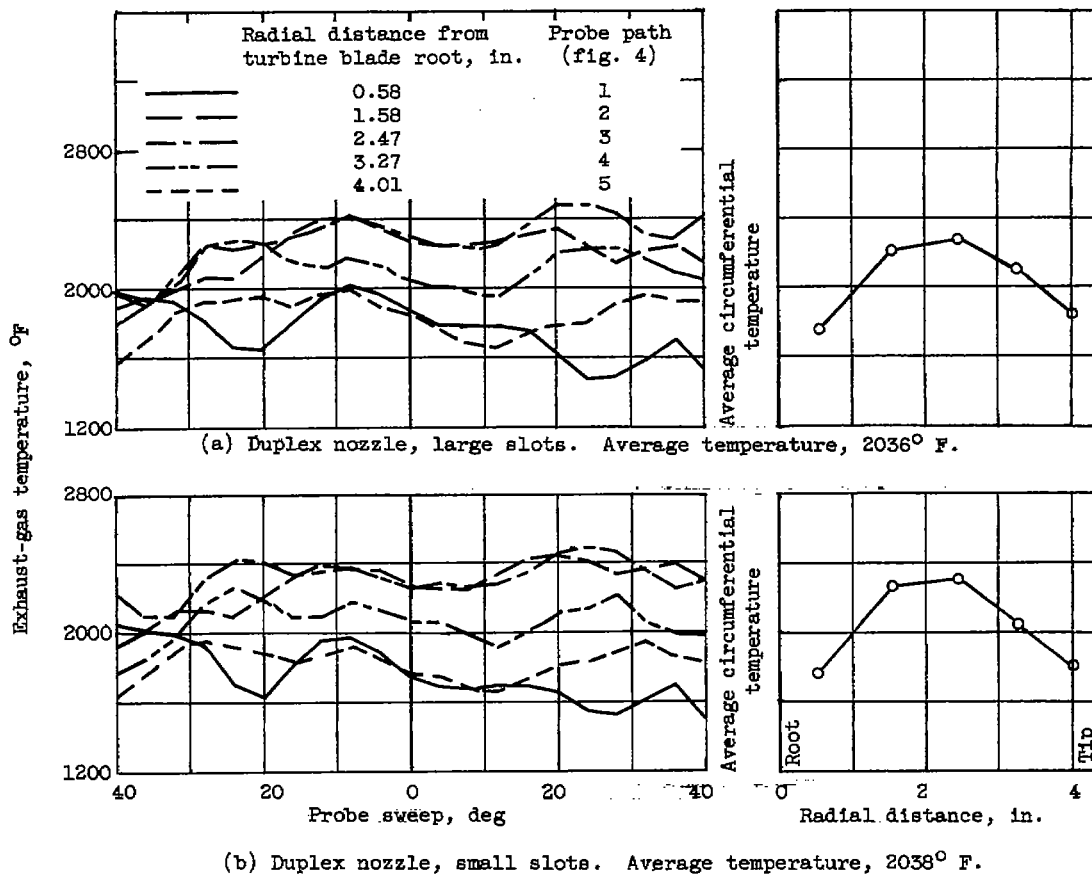
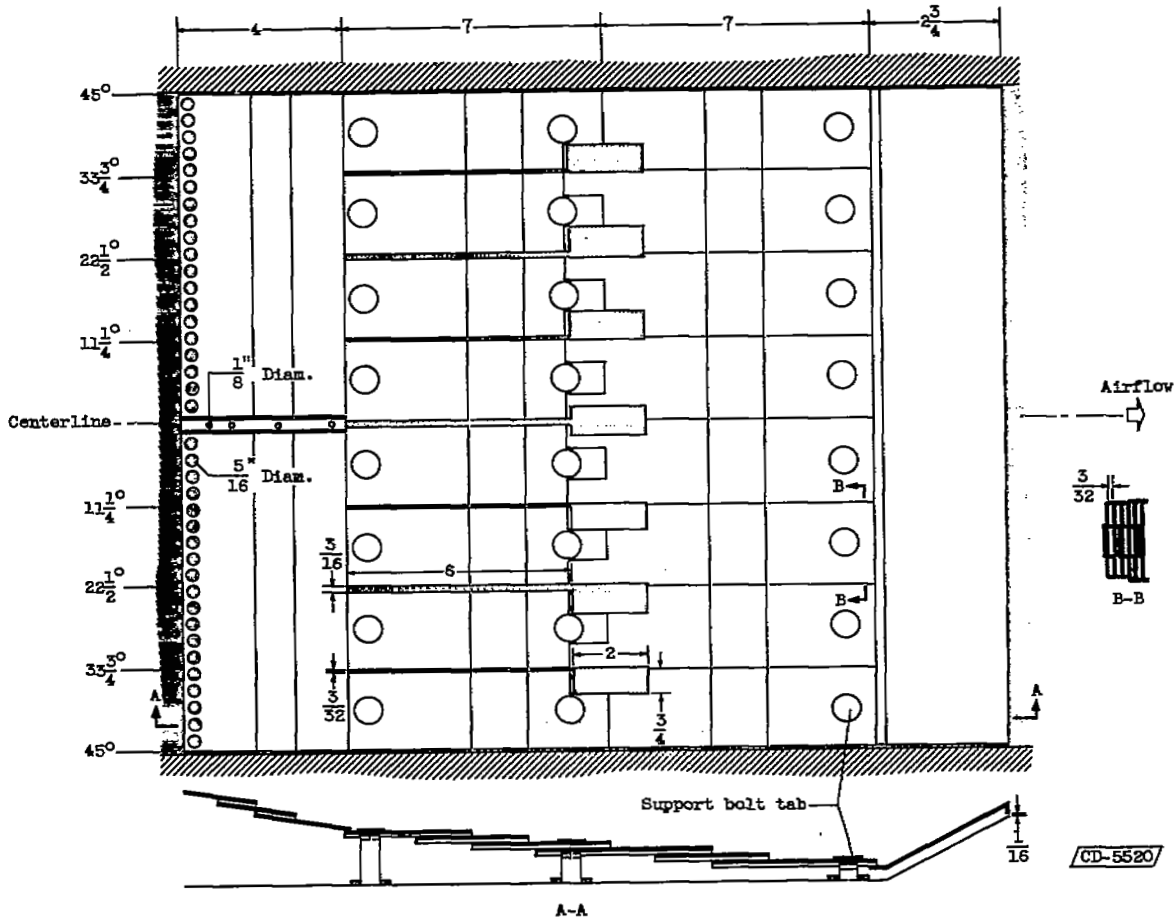


Figure 22. - Exhaust-gas temperature patterns for configuration 20. Test condition B.

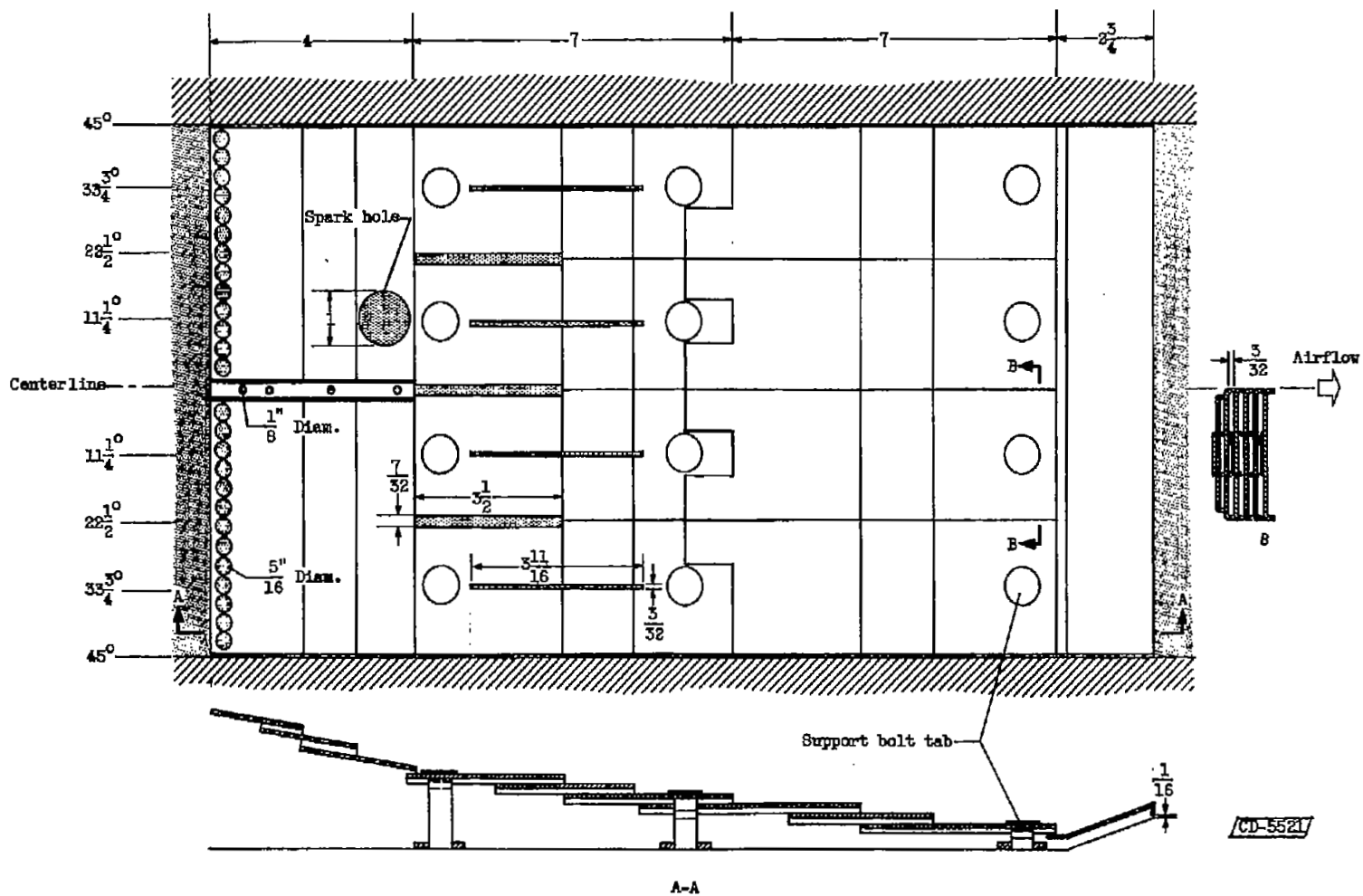
4378

CR-7 back



(a) Outer liner wall as viewed from flame zone.

Figure 23. - Schematic layout and dimensions of air-admission area of configuration 20. (All dimensions in inches.)



(b) Inner liner wall as viewed from flame zone.

Figure 23. - Concluded. Schematic layout and dimensions of air-admission area of configuration 20.
(All dimensions in inches.)

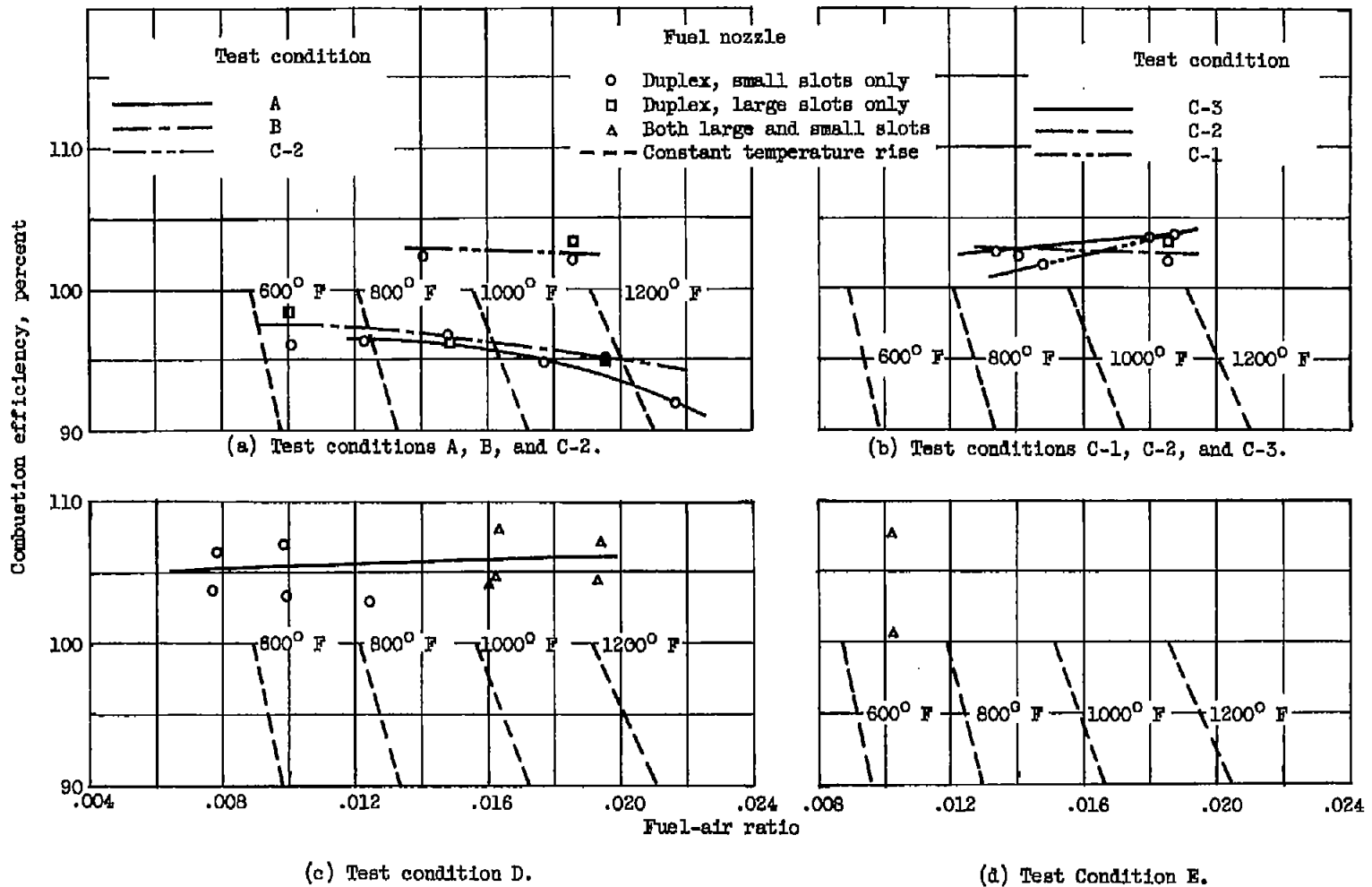
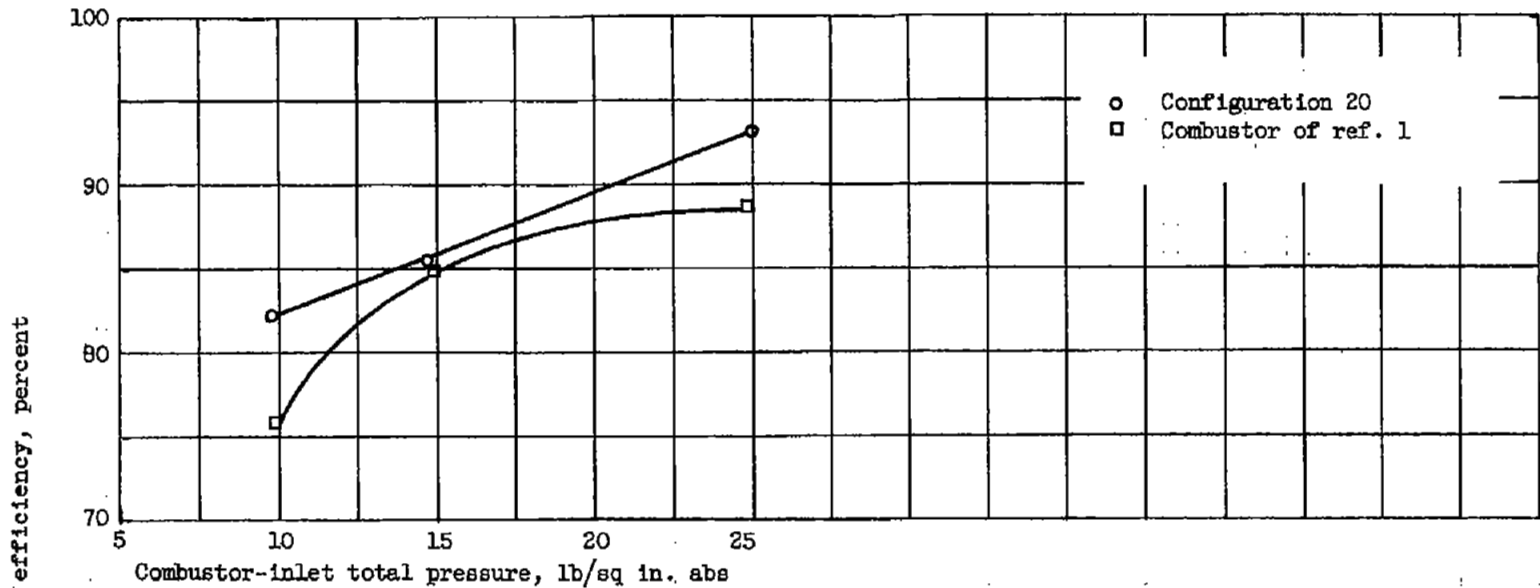
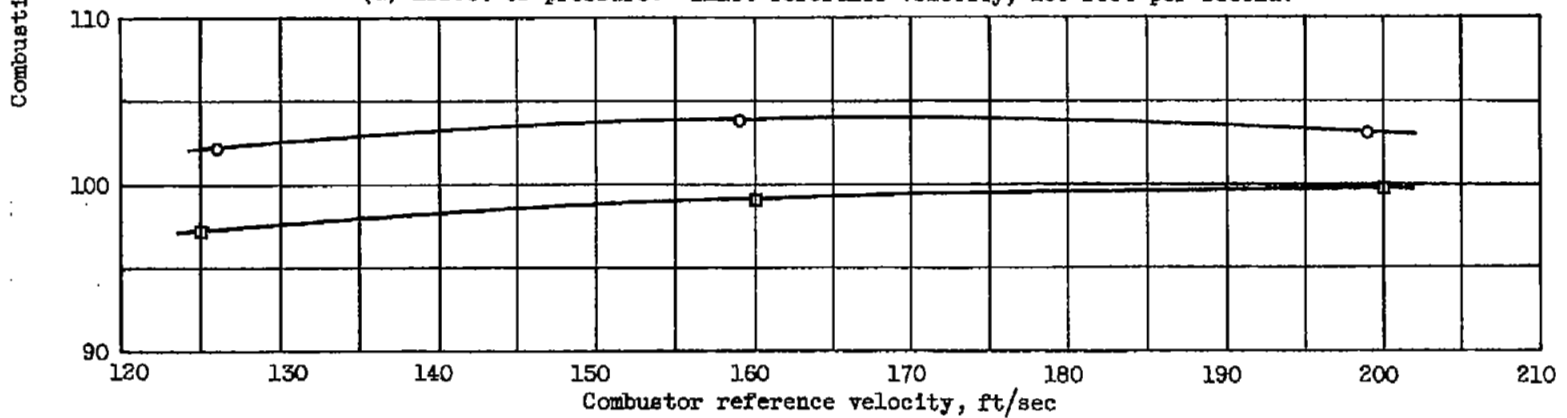


Figure 24. - Variation in combustion efficiency with fuel-air ratio for configuration 20 at all conditions tested.



(a) Effect of pressure. Inlet reference velocity, 160 feet per second.



(b) Effect of velocity. Inlet pressure, 25 pounds per square inch absolute.

Figure 25. - Comparison of combustion efficiency for configuration 20 and combustor from reference 1 at average exhaust temperature of about 2000° F. Inlet-air temperature, 860° F.

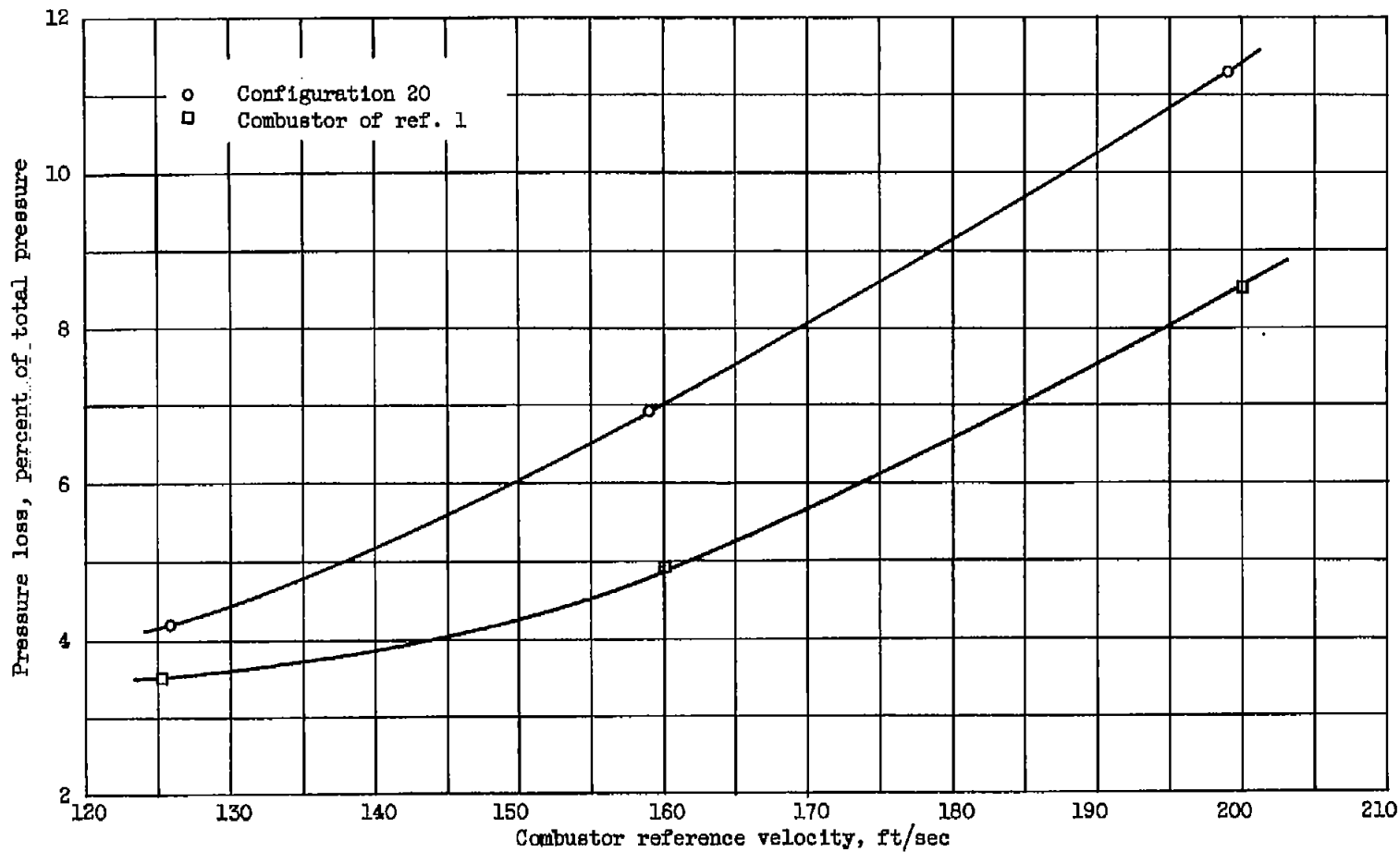


Figure 26. - Comparison of pressure loss for configuration 20 and combustor from reference 1 for a range of reference velocities. Inlet pressure, 25 pounds per square inch absolute; inlet temperature, 860° F; average exhaust temperature, about 2000° F.

UNCLASSIFIED

NASA Technical Library



3 1176 01436 5713

UNCLASSIFIED

~~CONFIDENTIAL~~